Biogeochemistry (2006) 77: 375–408
DOI 10.1007/s10533-005-1640-1
© Springer 2006

Porewater stoichiometry of terminal metabolic products, sulfate, and dissolved organic carbon and nitrogen in estuarine intertidal creek-bank sediments

NATHANIEL B. WESTON[1,2], WILLIAM P. PORUBSKY[1], VLADIMIR A. SAMARKIN[1], MATTHEW ERICKSON[1], STEPHEN E. MACAVOY[1,3] and SAMANTHA B. JOYE[1,*]

*[1]Department of Marine Science, University of Georgia, Athens, GA, 30605, USA; [2]Current address: Patrick Center for Environmental Research, The Academy of Natural Sciences, Philadelphia, PA, USA; [3]Current address: Biology Department, American University, Washington, District of Columbia, USA; *Author for correspondence (e-mail:mjoye@uga.edu; phone: +1-706-542-6818; fax: +1-706-542-5888)*

Key words: Carbon, Dissolved organic carbon (DOC), Dissolved organic nitrogen (DON), Sediment metabolism, Nitrogen, Sulfate reduction

Abstract. Porewater equilibration samplers were used to obtain porewater inventories of inorganic nutrients (NH_4^+, NO_x, PO_4^{3-}), dissolved organic carbon (DOC) and nitrogen (DON), sulfate (SO_4^{2-}), dissolved inorganic carbon (DIC), hydrogen sulfide (H_2S), chloride (Cl^-), methane (CH_4) and reduced iron (Fe^{2+}) in intertidal creek-bank sediments at eight sites in three estuarine systems over a range of salinities and seasons. Sulfate reduction (SR) rates and sediment particulate organic carbon (POC) and nitrogen (PON) were also determined at several of the sites. Four sites in the Okatee River estuary in South Carolina, two sites on Sapelo Island, Georgia and one site in White Oak Creek, Georgia appeared to be relatively pristine. The eighth site in Umbrella Creek, Georgia was directly adjacent to a small residential development employing septic systems to handle household waste. The large data set (>700 porewater profiles) offers an opportunity to assess system-scale patterns of porewater biogeochemical dynamics with an emphasis on DOC and DON distributions. SO_4^{2-} depletion $(SO_4^{2-})_{Dep}$ was used as a proxy for SR, and $(SO_4^{2-})_{Dep}$ patterns agreed with measured (^{35}S) patterns of SR. There were significant system-scale correlations between the inorganic products of terminal metabolism (DIC, NH_4^+ and PO_4^{3-}) and $(SO_4^{2-})_{Dep}$, and SR appeared to be the dominant terminal carbon oxidation pathway in these sediments. Porewater inventories of DIC and $(SO_4^{2-})_{Dep}$ indicate a 2:1 stoichiometry across sites, and the C:N ratio of the organic matter undergoing mineralization was between 7.5 and 10. The data suggest that septic-derived dissolved organic matter with a C:N ratio below 6 fueled microbial metabolism and SR at a site with development in the upland. Seasonality was observed in the porewater inventories, but temperature alone did not adequately describe the patterns of $(SO_4^{2-})_{Dep}$, terminal metabolic products (DIC, NH_4^+, PO_4^{3-}), DOC and DON, and SR observed in this study. It appears that production and consumption of labile DOC are tightly coupled in these sediments, and that bulk DOC is likely a recalcitrant pool. Preferential hydrolysis of PON relative to POC when overall organic matter mineralization rates were high appears to drive the observed patterns in POC:PON, DOC:DON and DIC:DIN ratios. These data, along with the weak seasonal patterns of SR and organic and inorganic porewater inventories, suggest that the rate of hydrolysis limits organic matter mineralization in these intertidal creek-bank sediments.

Introduction

Coastal regions account for the majority of organic matter mineralization in marine sedimentary environments (Middelburg et al. 1997). Benthic-pelagic processes are tightly coupled in shallow coastal systems (Rowe et al. 1976), and sediment remineralization of organic matter provides a significant fraction of the inorganic nutrients required to support benthic and water-column primary production (Boynton and Kemp 1985; Hopkinson et al. 1999). The mineralization of particulate organic matter (POM) in anaerobic sediments is achieved largely by the coupling of hydrolytic, fermentative and terminal metabolic processes (Figure 1, Fenchel and Findlay 1995). Dissolved organic matter (DOM) formed by the initial hydrolysis of POM is subsequently oxidized to inorganic end products by fermenters and terminal metabolizers (Figure 1).

Despite the importance of DOM as an intermediate in the degradation of organic matter, relatively little is known about DOM dynamics in estuarine

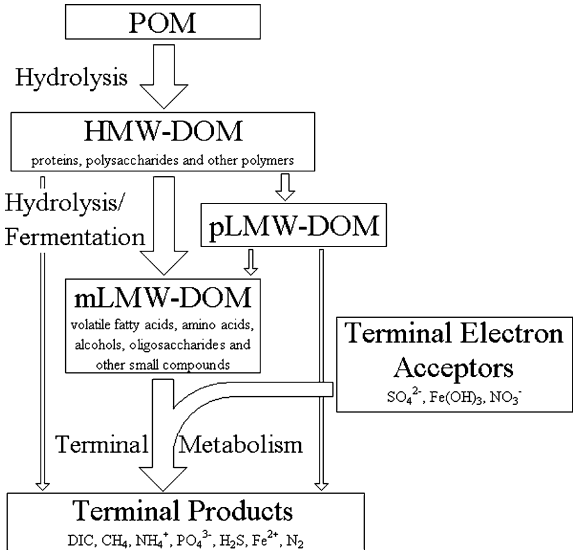

Figure 1. Conceptual diagram of the breakdown of organic matter in anaerobic sediments (modified from Burdige and Gardner 1998). Particulate organic matter (POM) is initially hydrolyzed to high molecular weight dissolved organic matter (HMW-DOM), which is then further hydrolyzed and fermented to monomeric low molecular weight dissolved organic matter (mLMW-DOM). The terminal oxidation of mLMW-DOM is coupled to the reduction of terminal electron acceptors [largely sulfate (SO_4^{2-}) in marine systems, but also iron oxides (such as $Fe(OH)_3$) and nitrate (NO_3^-)], producing dissolved inorganic carbon (DIC), methane (CH_4), ammonium (NH_4^+) and phosphate (PO_4^{3-}) as terminal end products of organic matter mineralization, as well as hydrogen sulfide (H_2S), reduced iron (Fe^{2+}) and dinitrogen gas (N_2) as the reduced forms of the electron acceptors. Some fraction of HMW-DOM is degraded into polymeric low molecular weight dissolved organic matter (pLMW-DOM) which is largely refractory and unavailable to the sediment microbial community.

sediments. Seasonal concentrations of porewater dissolved organic carbon (DOC) in Chesapeake Bay and Cape Lookout Bight sediments were similar and, in general, concentrations were positively correlated with temperature (Alperin et al. 1994; Burdige 2001). Molecular size determination studies of sediment DOC suggest that a small pool of polymeric low molecular weight DOC is produced in sediments and is recalcitrant to further remineralization (Amon and Benner 1996; Burdige and Gardner 1998). The bulk of labile DOM, however, is degraded to monomeric low molecular weight DOM that is then mineralized via terminal metabolic processes (Figure 1).

Much less is known about dissolved organic nitrogen (DON) dynamics in estuarine sediments. Due to the importance of nitrogen in regulating coastal system productivity (Howarth 1988), the concentrations and fate of DON in coastal sediments is relevant and potentially significant. Sediment cycling of specific fractions of DON such as amino acids (Burdige and Martens 1988) and urea (Lomstein et al. 1989) have been investigated, as have sediment DON flux rates (Hopkinson 1987; Enoksson 1993; Burdige and Zheng 1998). However, porewater profiles of total DON are sparse (Enoksson 1993; Burdige and Zheng 1998; Yamamuro and Koike 1998).

In the current study, we document seasonal and spatial patterns of DOC and DON along with, and in relation to, several other biogeochemical variables in shallow intertidal estuarine sediments at eight sites in coastal South Carolina and Georgia. Sediment porewater profiles were measured in porewater equilibration samplers to obtain seasonal steady-state inventories of DOC, DON, ammonium (NH_4^+), nitrate + nitrite (NO_x), phosphate (PO_4^{3-}), dissolved inorganic carbon (DIC), reduced iron (Fe^{2+}), chloride (Cl^-), sulfate (SO_4^{2-}), hydrogen sulfide (H_2S) and methane (CH_4) at sites across gradients in salinity in several estuarine systems. A large data set of over 700 individual profiles was obtained. A more limited amount of sediment solid phase particulate organic carbon (POC) and nitrogen (PON) pool size determinations and SO_4^{2-} reduction (SR) rate measurements were also made.

This study provides a comprehensive description of system-scale patterns of sediment biogeochemistry with emphasis on DOC and DON in intertidal creek-bank environments. Rather than focus on metabolic pathways and nutrient and organic matter dynamics at any one site, we chose to evaluate patterns at the system-scale. A site that appears to receive septic inputs from the adjacent residential community is discussed in more detail.

Methods

Study site

Eight sites in coastal Georgia and South Carolina, USA, were used to investigate shallow estuarine sediment processes (Figure 2). We chose to investigate porewater biogeochemistry of intertidal creek-bank sediment in relatively small

tidal creeks. These intertidal sites were macrophyte free, but benthic microalgae were present on the sediment surface at most sites. The salt marsh vegetation adjacent to the creek-bank was dominated by *Spartina alterniflora* at all sites.

Sites on the Duplin River (SAP1) and Dean Creek (SAP2) were sampled on Sapelo Island, Georgia. These pristine marsh sites are saline, but can be influenced by freshwater discharge from the Altamaha River. Two sites in the Satilla River estuarine system were also sampled. Site STL1 is in the White Oak Creek tributary to the Satilla River, and site STL2 is adjacent to the Dover Bluff residential community, and may receive septic inputs from the developed

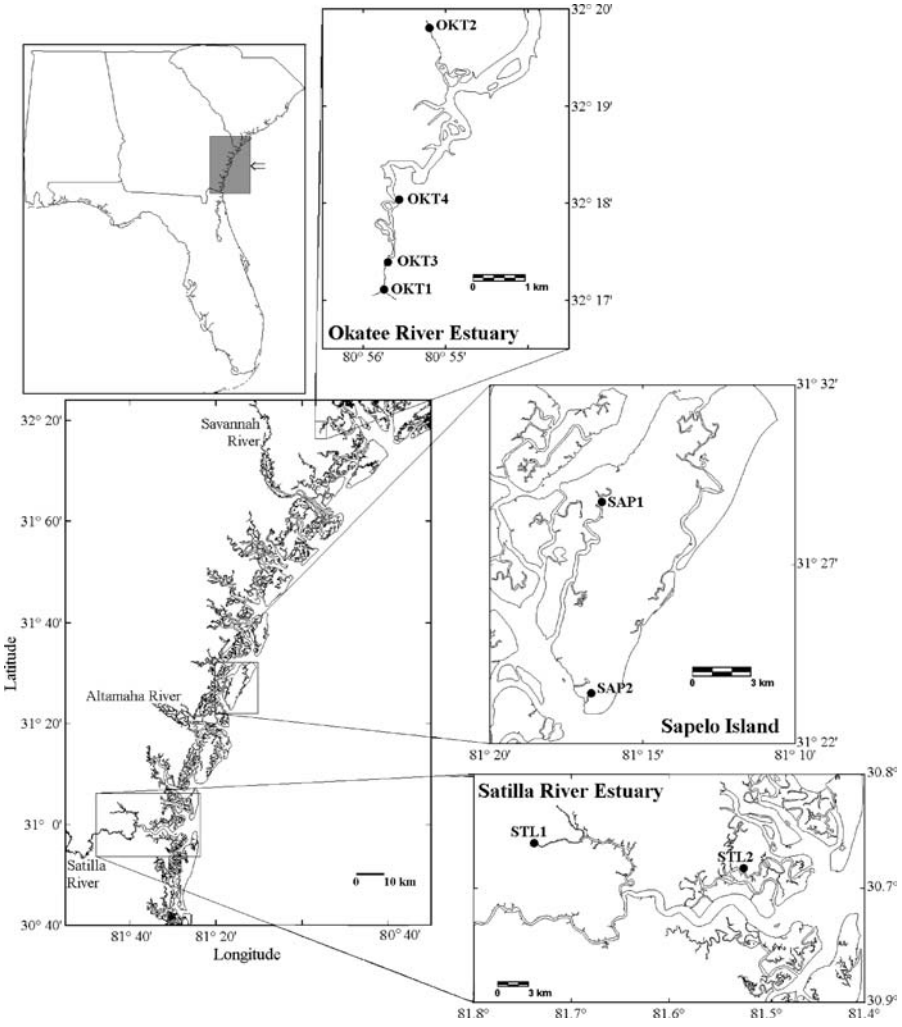

Figure 2. Map of the sampling sites in the Okatee River Estuary (South Carolina), Sapelo Island and Satilla River Estuary (Georgia).

upland. The STL2, SAP1 and SAP2 sites were sampled between September 2000 and August 2003 (Table 1). STL1, sampled in 2002 and 2003, is an oligohaline site upstream from site STL2.

Four sites in the Okatee River Estuary system (Figure 2) in South Carolina, a mid-sized tidal creek draining into the Colleton River Estuary, were sampled between 2001 and 2003 (Table 1). Sites OKT1, OKT3 and OKT4 were sampled along a salinity gradient in the Okatee Estuary. Salinity in the Okatee is highly dependent on freshwater discharge. Site OKT1 in the upper reaches of the Okatee can have salinities ranging from 0 to 20 ppt. The OKT4 site further downstream in the Okatee is less influenced by freshwater discharge, with salinities typically near seawater levels. The OKT2 site on Malind Creek, a small tidal creek feeding the Okatee, typically has salinities comparable to the OKT1 site. In January 2003, an additional five sites between the OKT3 and OKT4 sites were sampled to evaluate spatial variability in porewater biogeochemistry (Table 1).

Experimental design

Porewater was sampled using porewater diffusion equilibration samplers (hereafter referred to as 'peepers', Hesslein 1976), constructed from ultra high molecular weight polyethylene. Thirty 18 ml volume chambers (12 cm wide $\times$ 1 cm in height $\times$ 1.5 cm in depth) were machined at 1.5 or 2.0 cm intervals into a back-plate ($14 \times 60 \times 2$ cm), over which a 0.2 μm nylon membrane (Biotrans® Nylon Membrane) and a 0.5 cm thick cover-plate (with openings,

Table 1. Schedule of porewater equilibration meter sampling, sediment solid phase POC and PON measurement and sulfate reduction (SR) rate determination at the Georgia and South Carolina field sites.

Date	Georgia	South Carolina
Porewater equilibration samplers		
September 2000	STL2, SAP1, SAP2	
January 2001	STL2, SAP1, SAP2	
April 2001	STL2, SAP1, SAP2	OKT1
August 2001[a]	STL2, SAP1, SAP2	OKT4, OKT3
January 2002	STL2, SAP1, SAP2	OKT1, OKT3, OKT4, OKT2
August 2002	STL2, SAP1, SAP2, STL1	OKT1, OKT3, OKT4, OKT2
January 2003	STL2, STL1	OKT1, OKT3, OKT4, OKT2, Survey[b]
POC, PON, and SR		
April 2002	STL2, SAP1, SAP2	OKT4, (OKT1, OKT3)[c]
June 2002	STL2	OKT4
August 2002	STL2, SAP2	OKT4
January 2003	STL2	OKT4

Abbreviations correspond to sites in (Figure 2).
[a]Single porewater equilibration meter at each site during August 2001.
[b]Single meter at five survey sites between the OKT3 and OKT4 sites (Figure 2).
[c]Sediment solid phase measurements only.

corresponding to the chambers) were placed and secured with natural nylon screws. Assembly was conducted with the sampler submerged in deionized water, with care taken to ensure the chambers were bubble free. Samplers were stored for at least five days in He purged deionized water prior to deployment.

Peepers were transported to the field sites in He purged deionized water, and duplicate peepers were deployed vertically in the unvegetated, intertidal creek-bank sediment at each site (with the exception of August 2001 and the survey sites when single peepers were deployed). At the OKT sites where creek-banks were generally steeper than at other sites, peepers were deployed at two heights on the creek-bank; one approximately 0.5 m below vegetation and the other at approximately mean low water. At the SAP and STL sites, peepers were deployed parallel to the creek at approximately 0.5 m below vegetation. Peepers were allowed to equilibrate for 6–8 weeks before collection. Peepers were deployed on seven dates at Georgia sites, and on three dates at South Carolina sites (Table 1). A total of 72 peepers were sampled at the eight sites (Table 1).

Ammonium (NH_4^+), nitrate + nitrite (NO_x), phosphate (PO_4^{3-}), dissolved organic carbon (DOC) and nitrogen (DON), dissolved inorganic carbon (DIC), hydrogen sulfide (H_2S), sulfate (SO_4^{2-}), chloride (Cl^-), reduced iron (Fe^{2+}), and methane gas (CH_4) were measured on the porewater inside the equilibration meter chambers. Additionally, intact sediment cores were obtained from the STL2 and OKT4 sites in April, June and August 2002 and January 2003 for particulate organic carbon (POC) and nitrogen (PON) analysis and *ex situ* SO_4^{2-} reduction rate assays using $^{35}SO_4^{2-}$ tracer.

Porewater analyses

Upon collection, peepers were immediately placed in thick (0.15 mm) polypropylene He purged bags and transported to the laboratory. In the lab, the peepers were placed in a He purged glove-bag (Aldrich® AtmosBag), and porewater in the chambers extracted into a gas-tight glass syringe after piercing the membrane with a needle (Becton-Dickinson® 18G) attached to the syringe and split into several containers for various analyses (Table 2).

All sample vials were acid-washed, rinsed with ultrapure water (Barnstead® NANOpure UV) and combusted at 500 °C prior to use. In the glove-bag, 1 ml of sample was injected into a He purged and crimp-sealed 6 ml headspace vial, which was then acidified with 0.1 ml of concentrated phosphoric acid for DIC (April 2001 and subsequent sampling dates) and CH_4 analysis. 1 ml of unfiltered sample was injected into a flow-through cell to determine pH (Sensorex model 450C electrode and FC49K flow cell). Unfiltered sample was pipetted into vials for alkalinity and H_2S determination. The remaining sample was then filtered through a 0.2 μm filter (Gelman® Acrodisk or Target® cellulose) into an 8 ml glass vial. Sample for NH_4^+ (0.1–0.5 ml) and for DOC, PO_4^{3-}, Cl^-,

Table 2. Treatment of the subsamples (filtered or unfiltered, volume, vial and preservation technique) taken from porewater equilibration chambers for various biogeochemical analyses.

Analysis	Sample	Volume (ml)	Vial	Preservation
CH_4, DIC[a]	Unfiltered	1	6 ml headspace vial with rubber septa and aluminum crimp seal	0.1 ml concentrated phosphoric acid
Alkalinity[b]	Unfiltered	0.1	7 ml glass vial	3 ml bromophenol blue reagent[‡], analyzed within 2 h
H_2S	Unfiltered	0.1–0.5	7 ml glass vial	0.5 ml 20% zinc acetate[‡]
NH_4^+	0.2 μm filtered	0.1–0.5	7 ml glass vial	0.2 ml phenol reagent[‡], analyzed within 2 days
NO_x, DON[c]	0.2 μm filtered	balance of sample	7 ml glass vial	Refrigerated
DOC[c], PO_4^{3-}, Cl^-, SO_4^{2-}, Fe^{2+}	0.2 μm filtered	4	7 ml glass vial	0.1 ml concentrated nitric acid, refrigerated

[a]Measured April 2001 and all subsequent samplings.
[b]September 2000 and January 2001 samples.
[c]Not measured on September 2000 samples; [‡]reagent added to sample vial prior to sampling.

SO_4^{2-}, and Fe^{2+} (4 ml sample + 0.1 ml of concentrated nitric acid) were then pipetted from this filtered sample (Table 2). The filtered sample remaining was saved for NO_x and TDN analysis. All vials were capped (teflon lined caps on NO_x/TDN and acidified samples) prior to removal from the glovebag. The reagents for NH_4^+, H_2S, and alkalinity were added to sample vials prior to sampling (Table 2).

Total alkalinity was measured immediately upon removal of vials from the glove-bag (Sarazin et al. 1999). NH_4^+ was analyzed within 2 days by standard colorimetric techniques (Solorazano 1969). NO_x (nitrate + nitrite) samples were refrigerated and analyzed within 2 weeks colorimetrically on an autoanalyzer (September 2000, January and April 2001 samples) by cadmium reduction, or vanadium reduction and nitric oxide (NO) detection on an Antek® chemiluminescent detector (745 NO_3^-/ NO_2^- reduction and 7050 NO analyzer, August 2001 and subsequent sampling dates). PO_4^{3-} was measured colorimetrically by autoanalyzer on acidified samples (Murphy and Riley 1962). SO_4^{2-} and Cl^- was determined by ion chromatography on a Dionex® DX 500 system on acidified samples. Fe^{2+} was determined on acidified samples using standard colorimetric techniques (Stookey 1970).

DIC (April 2001 and subsequent sampling dates) and CH_4 were analyzed on the gas phase of the acidified headspace vial after vigorous shaking. CH_4 and DIC were measured on a gas chromatograph equipped with a flame ionization detector (Shimadzu® GC 14A with 2 m Carbosphere column [Alltech® Instruments]) and a methanizer (Shimadzu®) to convert carbon dioxide to CH_4 for precise quantification. In September 2000 and January 2001, DIC was

calculated from total alkalinity and pH, after correction for the contribution of H_2S to the alkalinity (Stumm and Morgan 1996). Comparison between the two methods for determining DIC using a suite of sodium bicarbonate standards and porewater samples showed good agreement (<5% difference).

DOC was measured on a Shimadzu total organic carbon analyzer (TOC-5000®) on acidified (pH<2) samples after sparging with CO_2 free air for 15 min. Total dissolved nitrogen (TDN), and by difference the dissolved organic nitrogen (DON = TDN–[NH_4^+ + NO_x]), was analyzed by high-temperature catalytic oxidation of unacidified samples on a Shimadzu TOC machine coupled to an Antek® NO analyzer (Álvarez-Salgado and Miller 1998). As NH_3 is volatile and was lost from the TDN samples during storage, we found it necessary to re-measure the NH_4^+ concentration on these samples to correct for the change in NH_4^+ concentration. Filter (Gelman Acrodisk® and Target® cellulose filters) blanks for the dissolved organics were determined and corrected for. DOC filter blanks were significant when using the Gelman Acrodisk® filters, but were reproducible and thus easily corrected for. DON did not have measurable filter blanks.

Porewater profiles of each constituent were obtained, and the total sediment inventory was determined by integrating profiles by depth using trapezoidal approximation (correcting for porosity). Total inventory per cm^2 of sediment area was calculated to a depth of 40 cm, and for depths of 0–10 cm and from 10 to 40 cm. SO_4^{2-} depletion of the porewater inventories was calculated as

$$(SO_4^{2-})_{Dep} = [(Cl^-_{inv}) \cdot (R_{SW})^{-1}] - SO_4^{2-}{}_{inv} \quad (1)$$

where $(SO_4^{2-})_{Dep}$ is the SO_4^{2-} depletion of the inventory in μmol cm^{-2}, $Cl^-{}_{inv}$ and $SO_4^{2-}{}_{inv}$ are the measured Cl^- and SO_4^{2-} inventories in μmol cm^{-2}, respectively, and R_{SW} is the molar ratio of Cl^- to SO_4^{2-} in surface seawater (R_{SW} = 19.33).

$(SO_4^{2-})_{Dep}$ reflects the net amount of SO_4^{2-} consumption, presumably via SO_4^{2-} reduction, in the sediments. Cl^-, an unreactive anion is seawater, reflects the contribution of fresh versus saline waters in the porewater. As the concentrations of both Cl^- and SO_4^{2-} are orders of magnitude higher in seawater than in freshwater, the contribution of freshwater Cl^- and SO_4^{2-} to the inventories in the porewater is negligible, and freshwater dilutes seawater Cl^- and SO_4^{2-} concentrations. As the Cl^- to SO_4^{2-} ratio of seawater is constant (Pilson 1988), the 'expected' inventory of SO_4^{2-} can be calculated from the measured inventory of Cl^-. The observed (measured) SO_4^{2-} inventory is then subtracted from the 'expected' inventory, providing an estimate of SO_4^{2-} depletion, and thus net patterns of sulfate reduction, in the sediment column. DIC inventories were corrected for background overlying water DIC concentrations.

Between-site comparisons of seasonally averaged porewater inventories were conducted, and statistically different averages determined using analysis of variance and Tukey's pairwise comparison of means. In addition, inventories

of the measured porewater variables were regressed against average air temperature for the peeper deployment period (obtained from the National Climate Data Center, ncdc.gov), and corresponding porewater inventories of Cl^-, DIC and $(SO_4^{2-})_{Dep}$ at each site individually, and across all sites. The correlations between several other biogeochemical variables of interest were also explored. The carbon to $(SO_4^{2-})_{Dep}$ ($C{:}SO_4^{2-}$), carbon to nitrogen (C:N), and carbon to phosphorus (C:P) stoichiometries of organic matter mineralization in these estuarine sediments were estimated by regressing DIC against $(SO_4^{2-})_{Dep}$, NH_4^+ and PO_4^{3-} as well as $(SO_4^{2-})_{Dep}$ against NH_4^+ and PO_4^{3-}. The slopes of the linear best-fit regressions were corrected for the appropriate diffusion coefficients:

$$R = \left(\frac{\Sigma 1}{\Sigma 2}\right)\left(\frac{D_1}{D_2}\right) \tag{2}$$

where the stoichiometric ratio (R) equals the slope of the best-fit linear regression between two inventories ($\Sigma 1$ and $\Sigma 2$) multiplied by the appropriate diffusion coefficient ratio (D_1 and D_2). Diffusion coefficients for HCO_3^- (used for DIC), SO_4^{2-}, NH_4^+ and PO_4^{3-} were obtained from Boudreau (1997). The stoichiometric relationships SO_4^{2-}:N and SO_4^{2-}:P were multiplied by 2 to obtain estimates of C:N and C:P, respectively, assuming a $C{:}SO_4^{2-}$ ratio of 2 to 1 (Jørgensen 2000).

Solid phase and sulfate reduction rate measurements

POC and PON were measured at the STL2 and OKT4 sites on four dates (Table 1). Additionally, particulates were measured at the SAP1, SAP2, OKT1 and OKT3 sites in April 2002, and at the SAP2 site in August 2002. In January 2003, triplicate cores were obtained at the STL2 and OKT4 sites for POC and PON analysis to evaluate spatial variability. Intact sediment cores (7.8 cm inner diameter) were sectioned within two days of collection, and a known volume of sediment was dried at 80 °C to determine porosity and bulk density. Sediment was then ground, and both acidified (1 N HCl) and unacidified samples were analyzed on a ThermoFinnigan Flash EA 1112 Series NC analyzer to determine carbon and nitrogen content. Sediment POC content was determined for acidified samples (after removal of carbonates). Total sediment inventories of POC and PON were determined by trapezoidal integration. Additionally, the C:N ratio of organic matter undergoing mineralization was estimated from the best fit linear regression of POC against PON inventories at the two sites (OKT4 and STL2) for which adequate data was obtained.

Sulfate reduction (SR) rates were determined on four dates at the STL2 and OKT4 sites, and on two dates at the SAP2 site (Table 1). Triplicate sub-cores (0.8 cm inner diameter) were collected at 7 depths from intact sediment cores, capped with a rubber stoppers, and injected with 50 μl (about 2 μCi) of a $Na_2{}^{35}SO_4$ solution. Samples were incubated for 12 to 24 hours at *in situ*

temperatures and then transferred to 50 ml centrifuge tubes containing 10 ml of 20% zinc acetate solution to halt microbial activity and fix $H_2{}^{35}S$ as $Zn^{35}S$ and frozen. Samples were then centrifuged, and rinsed with N_2 purged distilled water and centrifuged several times to remove surplus $^{35}SO_4{}^{2-}$. The rinse water was saved to determine $^{35}SO_4{}^{2-}$ activity. The rinsed sediment was then subjected to a one-step hot chromous acid distillation to recover reduced ^{35}S (Canfield et al. 1986). The H_2S produced during the distillation was trapped in two in-line 5 ml zinc acetate traps. The activity of both the reduced sulfur and $SO_4{}^{2-}$ fractions was determined by scintillation counting (Beckman® LS 6500 scintillation system) of sample in ScintiSafe® Gel LSC Cocktail. The $SO_4{}^{2-}$ reduction rate was calculated as:

$$SR = ([{}^{35}S_{reduced}] \cdot [{}^{35}SO_4^{2-}]^{-1}) \cdot [SO_4^{2-}] \cdot \emptyset \cdot \alpha SO_4^{2-} \cdot t^{-1} \quad (3)$$

where the $SO_4{}^{2-}$ reduction rate (SR) rate is expressed as μmol $SO_4{}^{2-}$ reduced per cm^{-3} of sediment per day^{-1}, $[{}^{35}S_{reduced}]$ is the activity of the reduced sulfur pool, $[{}^{35}SO_4{}^{2-}]$ is the activity of the substrate pool added at the beginning of the experiment, $[SO_4{}^{2-}]$ is the pore water $SO_4{}^{2-}$ concentration (mM), $\emptyset$ is the sediment porosity, $\alpha SO_4{}^{2-}$ is the isotope fractionation factor for $SO_4{}^{2-}$ reduction (1.06; Jørgensen 1978), and t is incubation time (days). Total sediment rates (μmol cm^{-2} day^{-1}) were obtained by integrating the rate profile over depth, taking into account the porosity.

Results

A total of 72 sets of porewater profiles of $NH_4{}^+$, NO_x, $PO_4{}^{3-}$, DIC, DOC, DON, Fe^{2+}, Cl^-, $SO_4{}^{2-}$, H_2S and CH_4 were obtained at eight sites on several different dates (Table 1, Figure 2). Two profiles, from the STL2 and SAP1 sites in August 2002, are shown in Figure 3 as examples of the data obtained in this study. A subset of detailed data [Cl^-, DIC, $(SO_4{}^{2-})_{Dep}$ and $NH_4{}^+$] from duplicate porewater profiles at sites STL2 (an example of a diffusion-dominated site) and OKT3 (an example of a site at which advective flow appears to have effected porewater inventories) are shown in Figure 4. Due to the large number of individual profiles, seasonal and system-scale patterns are illustrated by the trends observed in depth-integrated porewater inventories.

Between-site comparisons

Comparison between sites was conducted on seasonally averaged porewater inventory data. The salinity gradients of the Georgia and South Carolina estuarine sites can be observed in the porewater Cl^- inventories. The seasonally averaged porewater inventories of Cl^- were lowest at the STL1 and OKT1 sites in Georgia and South Carolina, respectively, while the SAP2 and OKT4 sites had porewater Cl^- pools that approached full-strength seawater.

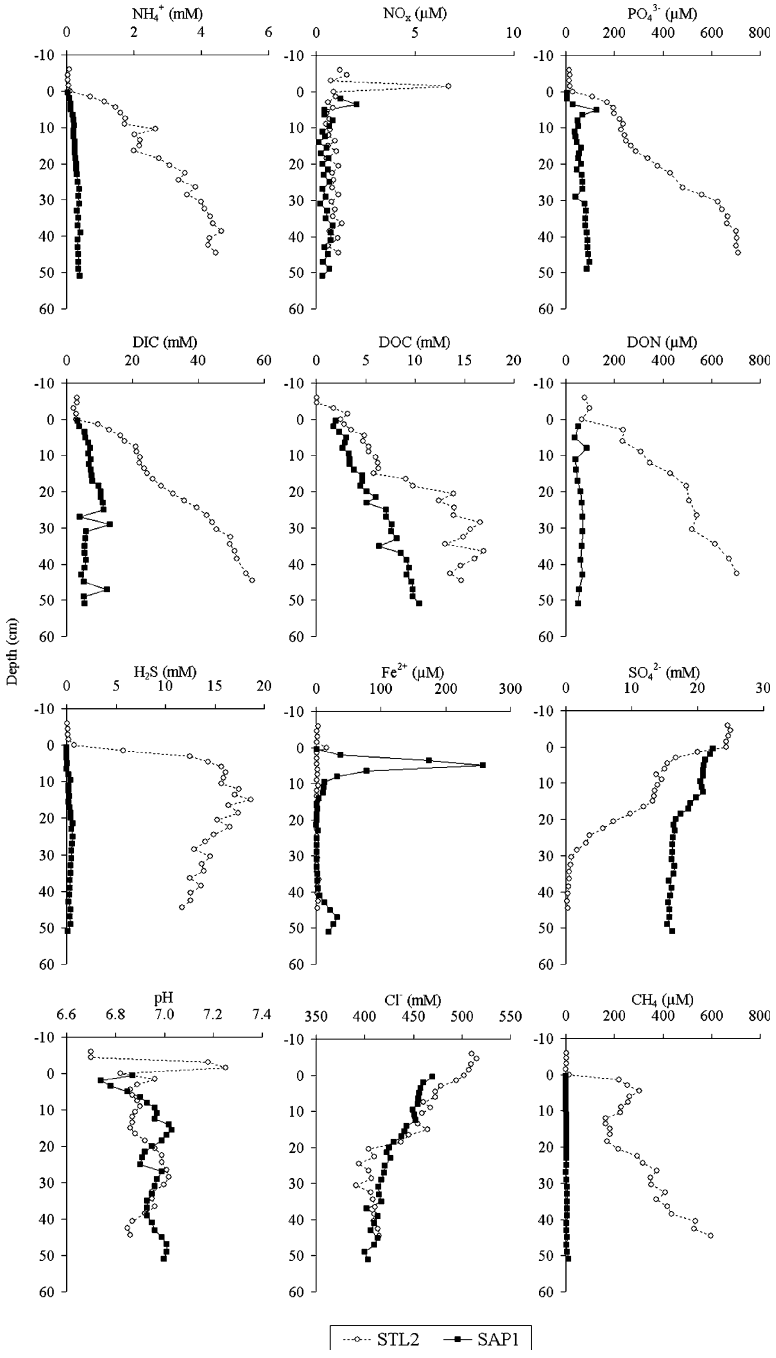

Figure 3. Example of porewater equilibration profiles of NH_4^+, NO_x, PO_4^{3-}, DIC, DOC, DON, H_2S, Fe^{2+}, SO_4^{2-}, pH, Cl^- and CH_4 (from the STL2 and SAP1 sites in August 2002).

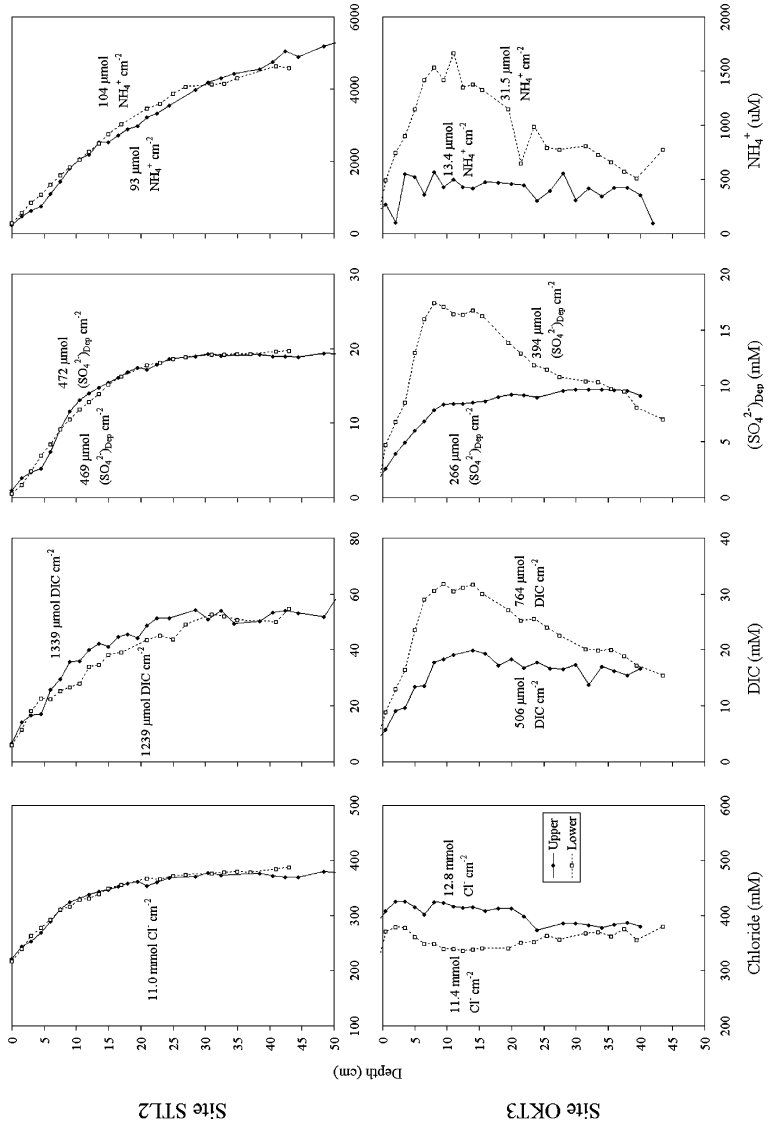

Figure 4. Example of duplicate porewater equilibration profiles of Cl^-, DIC, $(SO_4^{2-})_{Dep}$, and NH_4^+ from sites STL2 (January 2003) and OKT3 (August 2002). Porewater samplers were deployed parallel to the creek-bank at site STL2, and perpendicular to the creek-bank and at different heights below the marsh platform at site OKT3. The porewater inventory to 40 cm for each profile is indicated.

The STL2 site had significantly higher average porewater inventories of NH_4^+, PO_4^{3-}, DON, DIC and $(SO_4^{2-})_{Dep}$ (Equation 1) than any of the other sites ($p < 0.05$, ANOVA and Tukey pairwise comparison, Figure 5). Fe^{2+} inventories were higher at the SAP2 site than all sites except OKT2 ($p < 0.05$). There was no significant difference in the NO_x, DOC, H_2S, and CH_4 inventories between sites ($p > 0.05$), although the less saline sites (STL1, OKT1, OKT2) and the STL2 site did tend to have higher CH_4 (Figure 5).

System-scale patterns

Regressions between porewater inventories (0–10 and 10–40 cm) and average air temperature during the peeper deployment period and porewater inventories of Cl^- (Table 3), $(SO_4^{2-})_{Dep}$ and DIC (Table 4) were made to determine seasonality of and correlations between the various geochemical variables at each individual site (excluding the STL1 site and 'survey' sites due to small sample sizes). These regressions were also performed on data across all sites ('all sites'; Tables 3 and 4) with the exception of the STL2 site, due to the markedly different biogeochemical signature of this site (Figure 5).

$(SO_4^{2-})_{Dep}$ inventories from 0 to 40 cm were positively correlated with temperature at the SAP1, OKT3 and OKT2 sites, and in surface 10 cm at the STL2 and SAP1 sites. H_2S, NH_4^+ and PO_4^{3-} inventories also increased with warmer temperatures at several of the sites (Table 3). However, there was no significant correlation between DIC or CH_4 and temperature, and correlations between Fe^{2+} or DON and temperature were significant at only one site. DOC decreased with higher temperatures in the surface 10 cm at the SAP1 site only. When data were pooled for all sites excluding STL2, inventories of NH_4^+, $(SO_4^{2-})_{Dep}$, and H_2S in both surface (0–10 cm) and deep (10–40 cm) porewater was positively correlated with temperature (Table 3).

Seasonality was observed in the Cl^- pools, and this variability correlated with freshwater discharge to the coastal zone (Figure 6). Cl^- inventories were negatively correlated with the deployment period river discharge (data obtained from the United States Geological Survey) at the STL2, SAP1 and SAP2 sites in Georgia ($p < 0.05$, Altamaha River) and the OKT1 and OKT4 sites in South Carolina ($p < 0.05$, Savannah River, data not shown). There was little correlation between other measured variables and porewater inventories of Cl^-.

Higher inventories of DOC were measured at several OKT sites when porewater inventories of Cl^- were higher, while DON inventories decreased with Cl^- at the SAP1 site (Table 3). $(SO_4^{2-})_{Dep}$ to 40 cm was correlated with Cl^- inventories at the SAP2 site. At the SAP1 site, higher salinity sampling dates exhibited lower DIC and DON inventories, but increased $(SO_4^{2-})_{Dep}$ to 10 cm. CH_4 was negatively correlated with Cl^- inventories when data from all sites (excluding STL2) was pooled, and Fe^{2+} inventories were higher in 10–40 cm porewater (Table 3).

Porewater inventories of the measured biogeochemical variables were also compared with $(SO_4^{2-})_{Dep}$ and DIC inventories at each site (Table 4). Surface and deep inventories of NH_4^+ and PO_4^{3-} and $(SO_4^{2-})_{Dep}$ were positively correlated with DIC inventories at several of the sites, and DIC, NH_4^+ and PO_4^{3-} were likewise positively correlated with $(SO_4^{2-})_{Dep}$ at a number of sites

Table 3. Slopes of significant ($p < 0.05$) regressions of the measured porewater inventories (μmol cm^{-2}) from 0 to 10 cm and from 10 to 40 cm at each site (except STL1) against temperature (°C) and Cl^- inventories (mmol cm^{-2}).

Site	NH_4^+	NO_x	PO_4^{3-}	DIC	$(SO_4^{2-})_{Dep}$	CH_4	Fe^{2+}	H_2S	DON	DOC
Temperature										
10–40 cm										
STL2										
SAP1	0.158		0.024		2.931		−0.059	0.401		
SAP2									−0.294	
OKT1										
OKT2					8.11					
OKT3					12.36			15.71		
OKT4								12.50		
All sites	**0.33**				**3.25**			**5.12**		
10 cm										
STL2					3.228			3.432		
SAP1			0.010		0.788					−2.145
SAP2										
OKT1										
OKT2										
OKT3	0.347							3.164		
OKT4										
All sites	**0.072**				**0.703**			**0.492**		
Chloride										
10–40 cm										
STL2										
SAP1										
SAP2		−0.056			34.68					
OKT1							−1.846			12.87
OKT2			−0.451							
OKT3										16.15
OKT4										
All sites						**−0.967**	**0.310**			
10 cm										
STL2										
SAP1				−36.82	15.547				−0.784	
SAP2								−1.339		
OKT1										
OKT2										
OKT3										8.483
OKT4										20.707
All sites						**−0.184**				

'All sites' is data pooled from all sites with the exception of the STL2 site.

($p < 0.05$). There was also significant correlation between CH_4, Fe^{2+}, H_2S, DON and DOC with DIC or $(SO_4^{2-})_{Dep}$ at a few of the sites (Table 4).

Data pooled from all sites (except STL2) was also regressed against DIC and $(SO_4^{2-})_{Dep}$ inventories (Table 4, Figures 7 and 8). Inventories of NH_4^+, PO_4^{3-}, $(SO_4^{2-})_{Dep}$, CH_4 and H_2S were significantly positively correlated with DIC inventories at both 0–10 cm and 10–40 cm depths ($p < 0.05$, Table 4).

Table 4. Slopes of significant ($p < 0.05$) regressions of the measured porewater inventories (μmol cm^{-2}) from 0 to 10 cm and from 10 to 40 cm at each site (except STL1) against DIC and $(SO_4^{2-})_{Dep}$ inventories (μmol cm^{-2}).

Site	NH_4^+	NO_x	PO_4^{3-}	DIC	$(SO_4^{2-})_{Dep}$	CH_4	Fe^{2+}	H_2S	DON	DOC
DIC inventories										
10–40 cm										
STL2	0.102		0.010	NA	0.354	0.012	−0.001			−0.534
SAP1				NA						
SAP2				NA				0.046		
OKT1	0.021			NA	0.361			0.743		
OKT2	0.072			NA	0.333	0.047				
OKT3	0.031			NA	0.567					
OKT4			0.004	NA						
All sites	**0.026**		**0.004**	NA	**0.256**	**0.016**		**0.359**		
10 cm										
STL2	0.024		0.003	NA	0.154				0.005	
SAP1	0.011			NA					0.011	
SAP2			0.008	NA						
OKT1	0.017			NA						
OKT2	0.053		0.009	NA	0.491	0.027				
OKT3	0.052		0.013	NA	0.622				0.006	
OKT4				NA						
All sites	**0.037**		**0.011**	NA	**0.368**	**0.009**		**0.176**		
SO_4^{2-}*depletion inventories*										
10–40 cm										
STL2	0.236		0.026	2.309	NA	0.030				−1.445
SAP1			0.007		NA					
SAP2					NA					
OKT1	0.049			2.503	NA			1.992		
OKT2				1.972	NA					
OKT3	0.081			1.525	NA			0.937		
OKT4	0.094				NA					
All sites	**0.078**	**−0.001**	**0.010**	**1.842**	**NA**			**1.061**	**0.012**	
10 cm										
STL2	0.143		0.019	4.803	NA		−0.017		0.027	
SAP1					NA					−2.831
SAP2					NA					
OKT1					NA					
OKT2	0.103			1.842	NA					
OKT3	0.085		0.020	1.557	NA			0.763	0.009	
OKT4	0.122		0.036		NA			0.431		
All sites	**0.074**	**−0.001**	**0.019**	**1.334**	**NA**			**0.431**	**0.012**	

'All sites' is data pooled from all sites with the exception of the STL2 site.

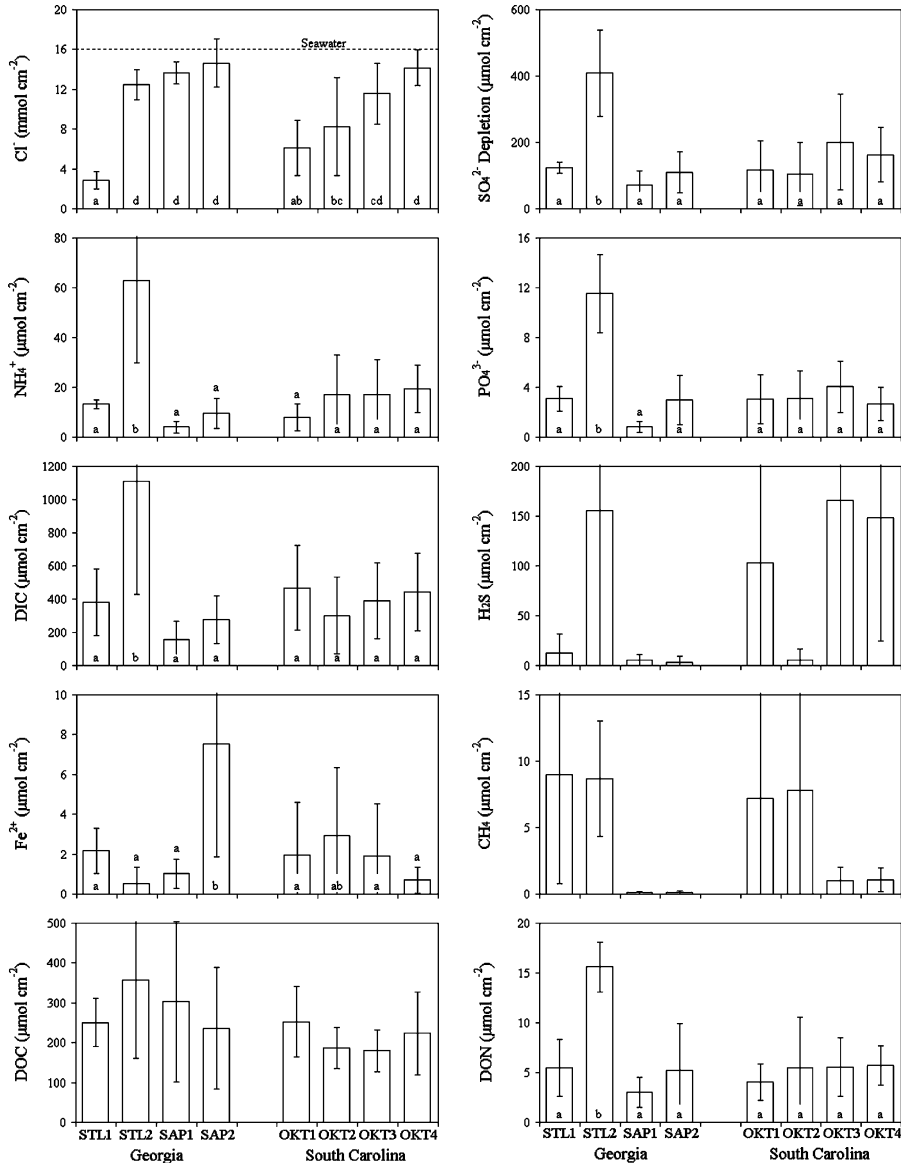

Figure 5. Seasonally averaged porewater inventories of Cl^-, $(SO_4^{2-})_{Dep}$, NH_4^+, PO_4^{3-}, DIC, H_2S, Fe^{2+}, CH_4, DOC and DON to a depth of 40 cm at eight sites in Georgia and South Carolina (± standard deviation). Sites that do not share the same letter are significantly different ($p < 0.05$, Tukey pairwise comparison).

Pools of DIC, NH_4^+, PO_4^{3-} (Figure 7), H_2S (not shown) and DON (Figure 8) were similarly positively correlated with $(SO_4^{2-})_{Dep}$ inventories, while NO_x inventories were negatively correlated to $(SO_4^{2-})_{Dep}$ pools (Table 4). The

slopes of NH_4^+ and PO_4^{3-} versus $(SO_4^{2-})_{Dep}$ were greater at the STL2 site compared to the 'all sites', while the DIC to $(SO_4^{2-})_{Dep}$ slopes were similar (Figure 7).

DOC was not significantly correlated with DIC or $(SO_4^{2-})_{Dep}$ ratios when data was pooled for all sites, but DOC decreased with increasing DIC and $(SO_4^{2-})_{Dep}$ at the STL2 site (Table 4, Figure 8). DON inventories were positively correlated with $(SO_4^{2-})_{Dep}$ for 'all sites' and, although DON at the STL2 site was not correlated with $(SO_4^{2-})_{Dep}$, the STL2 values fall in-line with the 'all sites' values (Figure 8). DON and DIC were not significantly correlated across sites, and CH_4 and Fe^{2+} were not correlated with either DIC or $(SO_4^{2-})_{Dep}$ inventories across sites (Table 4).

Molar ratios of DIN (NH_4^+) to DIP (PO_4^{3-}) inventories, when two outlying points were removed, were positively correlated with $(SO_4^{2-})_{Dep}$ ($p < 0.05$, Figure 9) for data pooled from all sites. A similar relationship was observed at the STL2 site ($p < 0.05$, Figure 9), although the increase in the DIN:DIP ratio with increasing $(SO_4^{2-})_{Dep}$ was slightly greater. DIC:DIN and DOC:DON ratios were highest at low $(SO_4^{2-})_{Dep}$, and decreased with increasing $(SO_4^{2-})_{Dep}$ [$p < 0.01$, log transformed $(SO_4^{2-})_{Dep}$, Figure 9]. These relationships were significant for all data pooled as well as when data from site STL2 was removed ($p < 0.01$).

There were several other noteworthy significant correlations between porewater inventories. Log-transformed Fe^{2+} and H_2S inventories (from 0 to 40 cm) were significantly negatively correlated [0–10 cm inventories: $\log(Fe^{2+}) = -0.25\log(H_2S) - 0.64$, $R^2 = 0.12$, $p < 0.01$; 10–40 cm inventories: $\log(Fe^{2+}) = -0.67\log(H_2S) + 0.17$, $R^2 = 0.57$, $p < 0.001$]. Inventories of Fe^{2+} did not exceed 3 μmol cm^{-2} unless H_2S inventories were below 20 μmol cm^{-2}.

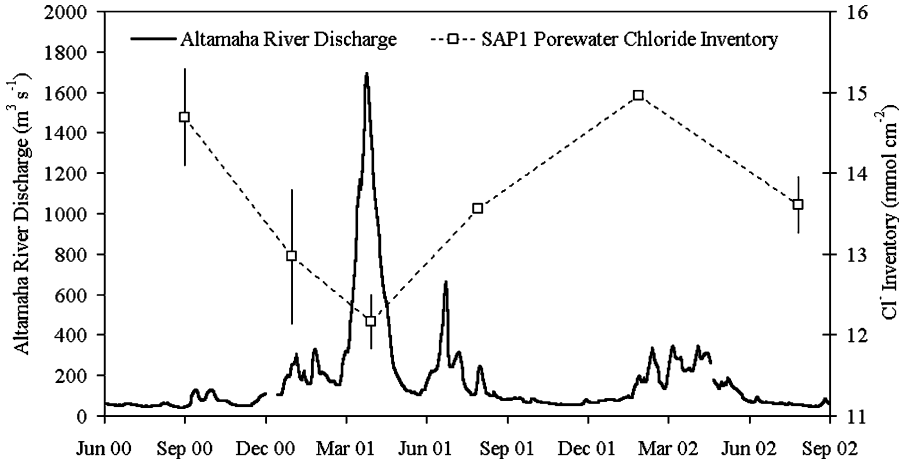

Figure 6. Altamaha River discharge (data from the United States Geological Survey) and porewater Cl^- inventories at the SAP1 site (±standard deviation except for August 2001).

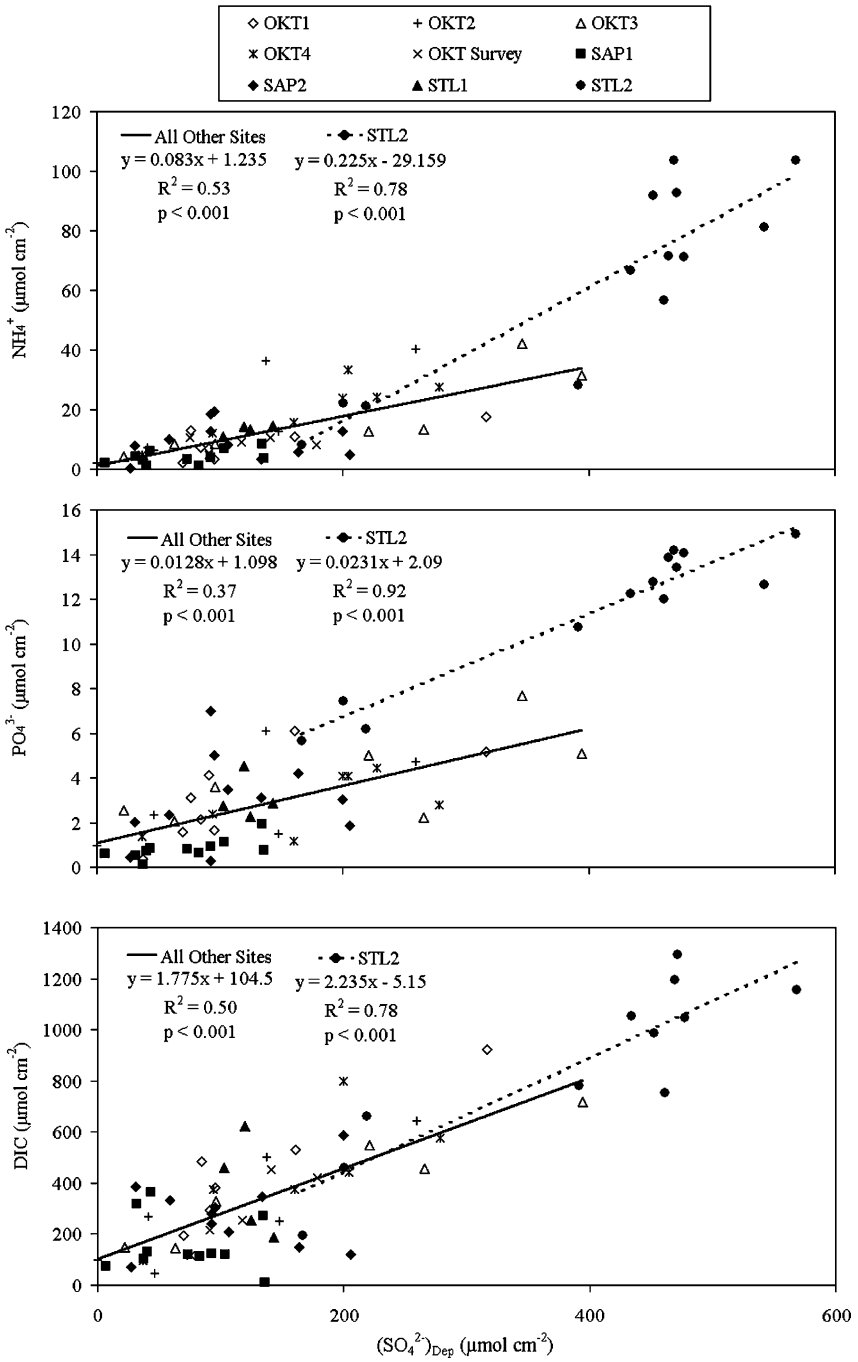

Figure 7. Sediment porewater inventories to 40 cm depth of NH_4^+, PO_4^{3-} and DIC against $(SO_4^{2-})_{Dep}$ inventories. Best-fit linear regressions are calculated for the STL2 site data separately from data from all of the other sites. Equations are given for significant relationships.

There was also a significant negative correlation between deep sediment inventories of Fe^{2+} and CH_4[$\log(CH_4) = -0.56\log(Fe^{2+}) - 0.56$, $R^2 = 0.26$, $p < 0.001$].

Sediment solid-phase and sulfate reduction rates

POC content ranged from 0.1 to 5.0 weight % and PON content from 0.05 to 0.8 weight % in these sediments. Sediment POM content was integrated with

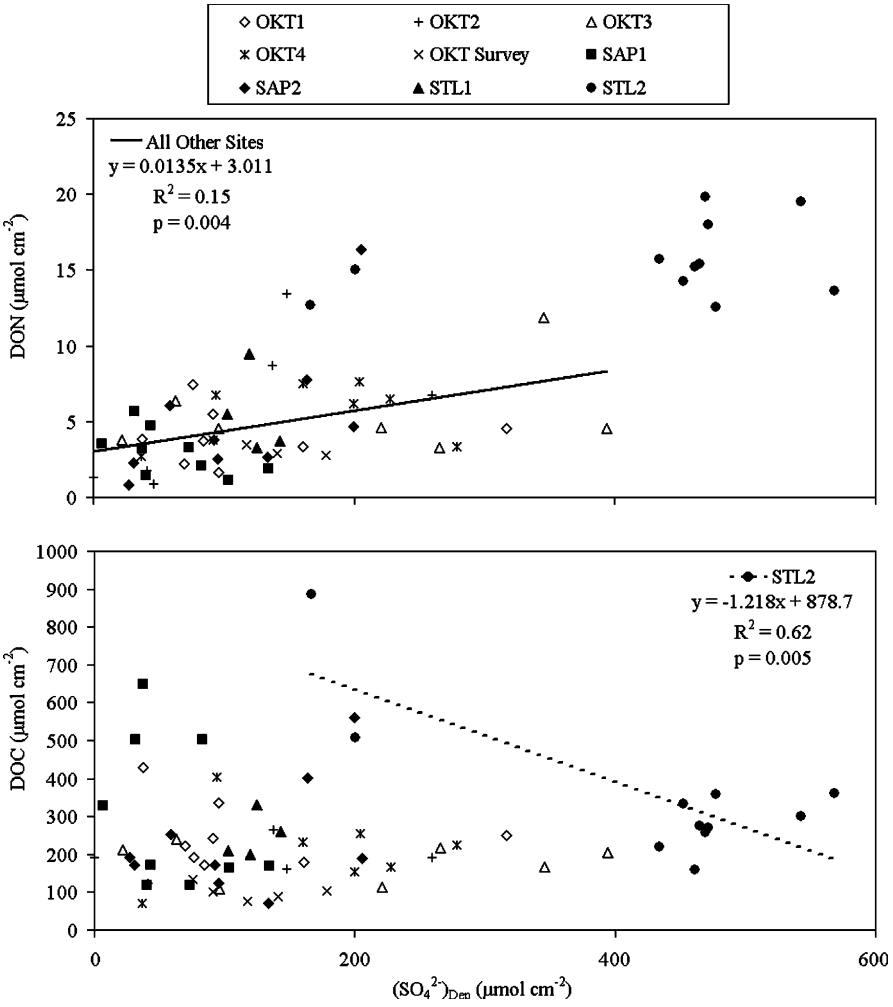

Figure 8. $(SO_4^{2-})_{Dep}$ inventories plotted against DON and DOC pools to 40 cm depth. Best-fit linear regressions are calculated for the STL2 site data separately from data from the other sites. Equations are given for significant relationships.

depth to 40 cm to obtain inventories of POC and PON (Table 5). There was not a clear difference in POM content between sites, although the SAP2 site had lower POC than the OKT4 and STL2 sites on two of the measurement dates. Molar ratios of POC:PON followed a very similar seasonal trend at the OKT4 and STL2 sites (Figure 10), increasing from April to a maximum in August, and subsequently decreasing into January.

Sulfate reduction rates generally decreased with depth in the sediment, although a shallow subsurface (5–10 cm) peak in activity was occasionally

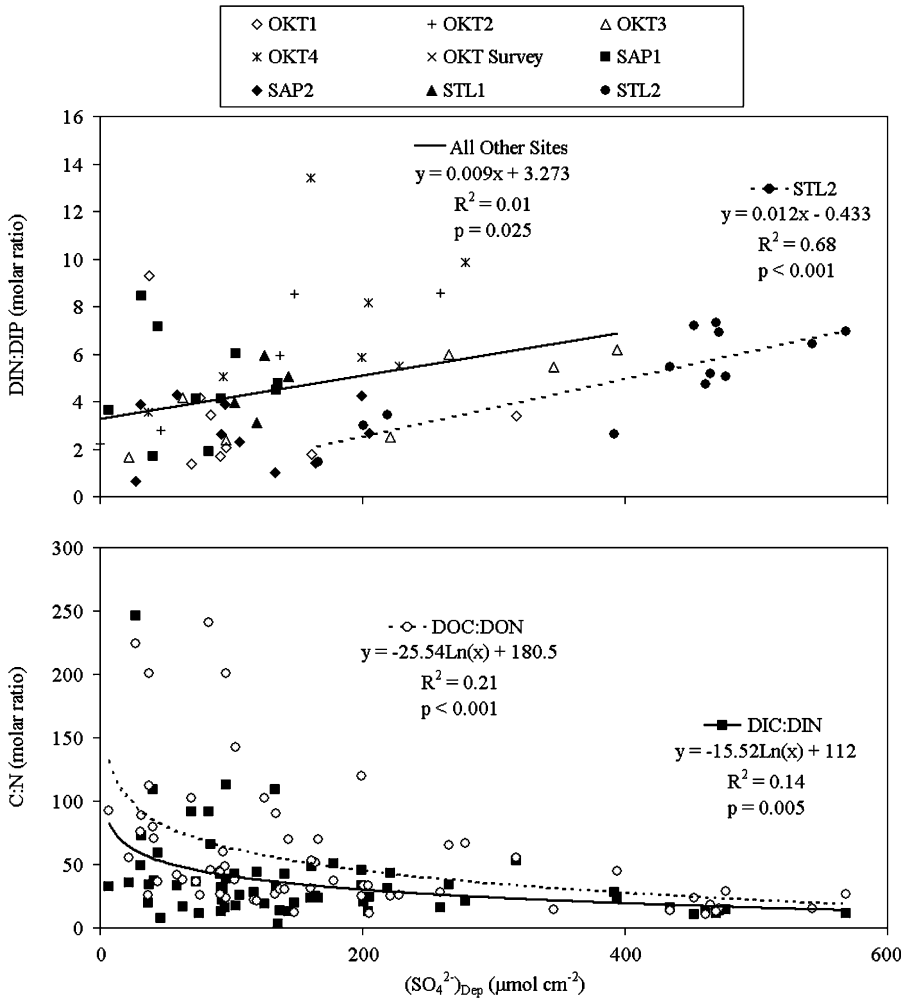

Figure 9. Molar ratios of DIN:DIP (top), DIC:DIN and DOC:DON (bottom) inventories versus sulfate depletion inventories to 40 cm. Best-fit linear regressions against log-transformed sulfate depletion inventories were made for the DIC:DIN and DOC:DON data (data pooled from all sites).

observed (data not shown). Integrated SR rates (to 40 cm) ranged from 0.3 to over 5 μmol cm^{-2} day^{-1} (Table 5). The STL2 site had higher rates of SO_4^{2-} reduction than the OKT4 and SAP2 sites, except in June 2002 (Table 5).

Stoichiometry of organic matter mineralization

Diffusion-corrected DIC to $(SO_4^{2-})_{Dep}$ ratios were 2.02 and 2.60 across all sites (except site STL2) and at site STL2 alone, respectively (Table 6). Estimates of the C:N ratio of mineralized organic matter ranged from 4 to 10, and C:P ratios ranged from 120 to 210 (Table 6). The C:N ratio at site STL2 was significantly lower (3.4–5.3) than at all other sites combined (7.6–10), as estimated using all three methods ($p < 0.05$, Table 6). The C:N stoichiometry as estimated from the POC to PON relationship (5.32) at site STL2 was significantly higher than the ratio estimated from $(SO_4^{2-})_{Dep}$ to NH_4^+ (3.41, $p < 0.05$, Table 6). There was considerably more overlap in the C:P ratios between all sites and site STL2, and differences were not significant ($p < 0.05$; Table 6).

Discussion

Over 70 sets of porewater profiles of nutrients (NH_4^+, NO_x and PO_4^{3-}), dissolved organics (DOC and DON), DIC, CH_4, Fe^{2+}, H_2S, Cl^- and SO_4^{2-} were integrated by depth to obtain porewater inventories at eights sites (Figure 2) on

Table 5. Sediment particulate organic carbon (POC) and nitrogen (PON) and sulfate reduction (SR) rates integrated to 40 cm depth.

Site	POC mmol cm^{-2}	PON mmol cm^{-2}	SR μmol cm^{-2} day^{-1}
April 2002			
STL2	51.9	5.0	5.2
SAP1	59.1	7.5	
SAP2	25.7	4.7	1.4
OKT1	39.3	6.1	
OKT3	30.8	5.5	
OKT4	43.6	4.4	0.9
June 2002			
STL2	56.3	4.1	2.1
OKT4	51.7	3.2	2.0
August 2002			
STL2	58.6	3.8	5.2
SAP2	22.5	2.7	2.0
OKT4	55.0	2.9	0.3
January 2003			
STL2	55.6	4.3	1.1
OKT4	46.8	3.9	0.4

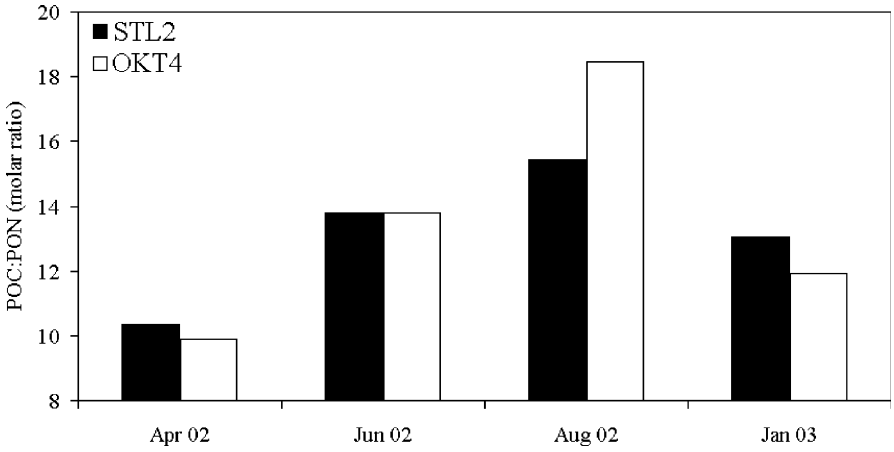

Figure 10. Particulate organic carbon (POC) to nitrogen (PON) molar ratios of sediment inventories to 40 cm at the STL2 and OKT4 sites on four dates.

several sampling dates (Table 1). The data discussed here offer a unique opportunity to assess spatial and temporal patterns of intertidal creek-bank sediment porewater stoichiometry and biogeochemistry in several estuarine systems.

Terminal metabolic pathways

Terminal oxidation of organic matter in sediments is coupled to the reduction of electron acceptors (Figure 1), the use of which depends on thermodynamic (relative energy yield) and kinetic (reactivity and availability) constraints (Froelich et al. 1979). Generally, aerobic respiration (O_2 reduction) is followed by denitrification (NO_3^-), metal reduction (manganese and iron oxides), SO_4^{2-} reduction, and finally methanogenesis (largely, acetate fermentation or CO_2 reduction). The variation in the net rates of terminal electron accepting processes over depth creates a biogeochemical zonation in sediments (Froelich et al. 1979). In coastal marine sediments and salt marshes, the availability of SO_4^{2-} relative to other terminal electron acceptors makes SO_4^{2-} reduction account for the majority of anaerobic carbon oxidation (Jørgensen 1982; Howarth 1993), although iron reduction can be an important pathway as well (Kostka et al. 2002a). In freshwater sediments, the low concentration of SO_4^{2-} results in the increased importance of methanogenesis (Capone and Kiene 1988) and iron reduction (Roden and Wetzel 1996).

Porewater inventories as measured in this study (Figure 5) were used to evaluate patterns and pathways of organic matter mineralization in intertidal estuarine sediments. The spatial scale of porewater inventories using data from

Table 6. Stoichiometry of organic matter mineralization estimated from slopes of porewater inventories (10–40 cm) of dissolved inorganic carbon (DIC) and sulfate depletion [$SO_4^{2-}{}_{(Dep)}$] against ammonium (NH_4^+) and phosphate (PO_4^{3-}) inventories and particulate organic carbon (POC) against particulate organic nitrogen (PON) at all sites except site STL2, and at site STL2 alone.

		DIC	$2[SO_4^{2-}{}_{(Dep)}]$[a]	POC
All sites				
($C:SO_4^{2-}$)	$SO_4^{2-}{}_{(Dep)}$	2.02 ± 0.29		
(C:N)	NH_4^+	9.98 ± 1.70	7.93 ± 0.92	
(C:N)	PON			7.59[b] ± 0.42
(C:P)	PO_4^{3-}	210.4 ± 41.2	150.4 ± 26.4	
Site STL2				
($C:SO_4^{2-}$)	$SO_4^{2-}{}_{(Dep)}$	2.60 ± 0.40		
(C:N)	NH_4^+	5.14 ± 0.66	3.41 ± 0.57	
(C:N)	PON			5.32 ± 0.40
(C:P)	PO_4^{3-}	161.2 ± 26.7	119.4 ± 12.1	

Slopes are derived from best-fit linear regressions(± standard error of regression), and have been corrected for appropriate diffusion coefficient ratios where appropriate.
[a]$SO_4^{2-}{}_{(Dep)}$ to NH_4^+ and PO_4^{3-} ratios have been doubled assuming a C: SO_4^{2-} ratio of 2.
[b]Site OKT4 only.

equilibration samplers, which provide a quasi steady-state profile, must be considered. Non-diffusive transport processes have the largest effect near the sediment–water interface in muddy sediments (bioturbation) or at depth along sedimentological discontinuities (e.g., sand layers). Intertidal creek-bank sediments in the study area are often populated by burrowing macrofauna (Teal 1958), which can enhance solute exchange between porewater and the overlying water (Meile et al. 2001). However, bioturbation affects mainly porewater concentrations in the upper 5 cm of sediment in intertidal estuarine sites (Meile et al. 2001), and very few burrows were observed on intertidal creekbank sediments during field sampling trips, with the exception of the SAP2 site.

The muddy estuarine sites we studied are largely diffusion-dominated even near the sediment-water interface. A detailed examination of the profiles obtained in this study suggested that the majority ($>90\%$) exhibited classical diffusive patterns (e.g. Figure 3 and site STL2, Figure 4). Nonetheless, it is difficult to state with absolute confidence that profiles are largely diffusive in nature and not influenced by bioturbation or advection. At the OKT sites, where peepers were placed perpendicular to the creek at different heights on the bank, the importance of advection in controlling profiles may be more readily apparent. A small subset of equilibration profiles did exhibit what appear to be advective signals (e.g. site OKT3, Figure 4), where the upper and lower peepers had variable chloride profiles that corresponded to variable profiles in other measured variables [DIC, $(SO_4^{2-})_{Dep}$ and NH_4^+]. These patterns were observed in relatively few peeper profiles, so we argue that the porewater equilibration inventories as presented in this paper represent the net metabolic processes occurring in the largely diffusion-dominated sediment column.

Porewater inventories reflect the balance between production/consumption and transport processes. Rapid turnover of substrates and products complicates the use of integrated inventories to identify dominant terminal electron accepting processes. Concentrations of substrates and/or products of several terminal electron-accepting processes are maintained at low concentrations in porewaters because of close coupling between processes. For instance, nitrification-denitrification may be closely coupled in the sediments, keeping NO_3^- concentrations low (Seitzinger 1988) and making NO_3^- inventories an unsuitable proxy for denitrification. CH_4 produced during methanogenesis may be subsequently oxidized anaerobically (Iversen and Jørgensen 1985) or aerobically (Sansone and Martens 1978), making CH_4 inventories a poor indicator of gross methanogenesis rates. Similarly, Fe^{2+} produced by iron reduction may be re-oxidized and/or precipitated, resulting in underestimates of iron reduction rates from Fe^{2+} inventories. In contrast, SO_4^{2-} concentrations in seawater are relatively high (millimolar levels), and although reoxidation of H_2S occurs in the sediment, sufficient drawdown of the SO_4^{2-} pool in sediments leads to significant change in SO_4^{2-} concentration with depth, and this depletion can be used to infer patterns of net SO_4^{2-} reduction.

We consider porewater inventories of $(SO_4^{2-})_{Dep}$ to be a proxy for patterns of net integrated SO_4^{2-} reduction rates in these estuarine sediments. Patterns of sulfate reduction measured with radiotracer methods agreed with patterns of $(SO_4^{2-})_{Dep}$ at the three sites where SO_4^{2-} reduction rate measurements were made (Figure 11), suggesting that variablility in $(SO_4^{2-})_{Dep}$ reflected rates of net SO_4^{2-} reduction at the sites rather than variability in transport or other processes. The slopes of the regressions between $(SO_4^{2-})_{Dep}$ and DIC inventories at several of the sites were close to 2 (Table 4, Figure 7), and when data was pooled across sites and corrected for variable diffusion, a DIC to

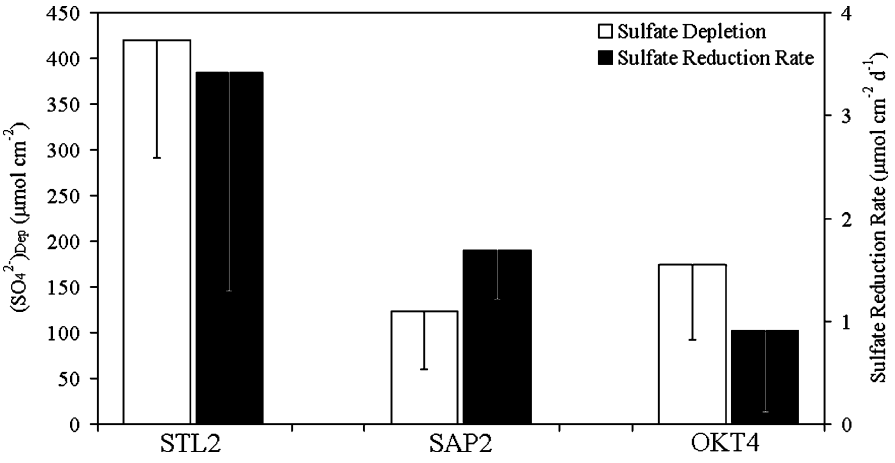

Figure 11. Seasonally averaged sulfate depletion inventories and depth-integrated sulfate reduction rates at the STL2, SAP2 and OKT4 sites (± standard deviation).

$(SO_4^{2-})_{Dep}$ ratio of 2 was observed (Table 6). The theoretical stoichiometry of SO_4^{2-} reduction coupled to the oxidation of organic matter:

$$2\ CH_2O + SO_4^{2-} \rightarrow 2\ HCO_3^- + H_2S \quad (4)$$

yields a SO_4^{2-} uptake to DIC release ratio of 2 (Jørgensen 2000), providing further evidence that sulfate reduction was the dominant pathway of anaerobic organic matter mineralization at these sites.

Depth-integrated sulfate reduction rate measurements (Table 5) are similar in magnitude to the benthic oxygen demand at several of the same sites, while measured rates of denitrification are orders of magnitude smaller (Porubsky et al. in Preparation). Because oxidation of reduced sulfur can account for a large fraction of the sediment oxygen demand (Jørgensen 1977), sediment SO_4^{2-} reduction may be as or more important than aerobic respiration in these intertidal creekbank sediments.

As mentioned previously, observations at the SAP2 site indicated a higher density of burrow networks than at other sites. Bioturbation can promote reoxidation of reduced compounds at depth in the sediment (Aller and Aller 1998), and may increase iron oxides available to iron reducing bacteria (Kostka et al. 2000a; Nielsen et al. 2003). Lowe et al. (2000) found large populations of iron reducing bacteria in surficial sediments at a site near the SAP2 site on Sapelo Island, and Kostka et al. (2000b) measured high rates of iron reduction in similar sediments. The SAP2 site Fe^{2+} inventories were the highest observed (Figure 5), suggesting that rates of microbial iron reduction may have been greater at this site than the other sites.

The relationships between the porewater inventories of several metabolic products (DIC, NH_4^+, PO_4^{3-}, H_2S) and inventories of $(SO_4^{2-})_{Dep}$ from sites across a range of salinities (Figure 5) and several different estuarine systems (Figure 2) are noteworthy (Tables 4 and 6, Figure 7). The magnitude of the inventories of $(SO_4^{2-})_{Dep}$ compared with NO_3^- (not shown), CH_4 and Fe^{2+} inventories (Figure 5) and the apparent coupling of the products of organic matter mineralization (DIC, NH_4^+, PO_4^{3-}, H_2S) with $(SO_4^{2-})_{Dep}$ (Figure 7, Tables 4 and 6) suggests that SO_4^{2-} reduction was the dominant pathway of anaerobic organic matter oxidation. However, the regulation of SO_4^{2-} reduction in these sediments was complex.

Spatial and temporal patterns

Temperature

There were seasonal temperature-driven variations in $(SO_4^{2-})_{Dep}$, NH_4^+, and H_2S inventories (Table 3). Rates of SO_4^{2-} reduction often follow a seasonal pattern similar to that of temperature in estuarine sediments and salt marshes (Jørgensen and Sørensen 1985; King 1988; Westrich and Berner 1988). Positive relationships between temperature and $(SO_4^{2-})_{Dep}$, H_2S and NH_4^+ suggests

that temperature contributes to the regulation of SO_4^{2-} reduction rates in these sediments. However, measured SO_4^{2-} reduction rates (Table 5) did not follow the expected seasonal pattern, and the correlation between temperature and porewater inventories was generally weak (Table 3). In short, temperature alone cannot explain the patterns documented here. Variation in the relative importance of pathways of organic matter oxidation (Kostka et al. 2002b), inherent small-scale variation in the estuarine creek-bank environment, and organic carbon availability to sulfate reducers (Westrich and Berner 1988, Marvin-DiPasquale and Capone 2003; V. Samarkin unpublished data) may also contribute to the observed patterns. Controls on organic matter mineralization will be discussed further in the "*System-Scale Patterns of DOM*" section.

Salinity

Salinity at these estuarine sites changed on seasonal timescales, corresponding to spring discharge events and increased river discharge to the coastal zone (Figure 6). Changes in porewater Cl^- did not appear to effect porewater pools of inorganic components (Table 3). Salinity influences the adsorption of NH_4^+ Rosenfeld (1979) and PO_4^{3-} (Sundareshwar and Morris 1999) to sediment particles. The magnitude of seasonal salinity changes at any one site, however, may not be sufficient to influence porewater NH_4^+ and PO_4^{3-} concentrations relative to other factors. Additionally, salinity can influence microbial processes such as nitrification and denitrification through direct inhibition (Rysgaard et al. 1999). Alternately, with increases in salinity, SO_4^{2-} concentrations increase, and sulfide produced from SO_4^{2-} reduction can inhibit nitrification (Joye and Hollibaugh 1995). We noted a slight but significant decrease of NO_x pools with increasing $(SO_4^{2-})_{Dep}$ inventories (Table 4), suggesting that net nitrification was lower when SO_4^{2-} reduction rates were high. However, coupled nitrification-denitrification occurs at the oxic-anoxic boundary in sediments (Seitzinger 1988), and in these estuarine sediments oxygen is depleted within a few mm (Joye et al., unpublished data). Additionally, porewater equilibration samplers may not have the depth resolution (1.5 cm intervals) to adequately capture the steep gradients at the depths where nitrification occurs. Nutrient dynamics are discussed further in the "*Inorganic N:P Ratios*" section.

Increased SO_4^{2-} availability associated with higher salinities also influences the balance between SO_4^{2-} reduction and methanogenesis, as methanogens are usually out-competed by SO_4^{2-} reducers for certain substrates when SO_4^{2-} is not limiting (Capone and Kiene 1988). There was, not surprisingly, a strong correlation between Cl^- and SO_4^{2-} inventories (data not shown), such that the less saline sites (STL1, OKT1 and OKT2) had significantly lower SO_4^{2-} than the more saline sites (SAP1, SAP2, OKT3 and SAP2). SO_4^{2-} concentrations declined with depth in porewaters at the less saline sites, and at the STL2 site, to SO_4^{2-} concentrations (<1 mM) that likely were limiting to SO_4^{2-} reducers (Roychoudhury et al. 1998). At the other saline sites, SO_4^{2-} concentrations did not limit SO_4^{2-} reducers. Methanogenesis at depth in the fresher (STL1, OKT1

and OKT2) and STL2 sites, due to SO_4^{2-} limitation of SO_4^{2-} reducers, resulted in a trend of higher CH_4 inventories. While this pattern was not evident seasonally at any single site, the effect of salinity on CH_4 inventories was apparent across sites independent of time (Table 3). The differences in CH_4 inventories between the fresh (and STL2) and saline sites were not significant due to high variability, but the fresher sites did have higher average CH_4 pools (Figure 5). These data suggests a larger fraction of organic carbon was oxidized via methanogenesis at the STL1, STL2, OKT1 and OKT2 sites where SO_4^{2-} availability limited the extent of SO_4^{2-} reduction.

Influence of development in the upland

The higher porewater inventories of $(SO_4^{2-})_{Dep}$, NH_4^+, PO_4^{3-}, DIC and DON at the STL2 site (Figure 5) clearly set this site apart from the other sites we studied. The STL2 site is adjacent to a residential community that utilizes septic systems to process household waste. Septic-derived materials may influence porewater concentrations and rates of microbial transformations at this site. Septic systems do not appear to efficiently process human waste, and septic-derived nutrient inputs can lead to the eutrophication of surface waters (Moore et al. 2003). Septic-derived waste also has high concentrations of inorganic nutrients and dissolved organic matter (Ptacek 1998).

The relationship between $(SO_4^{2-})_{Dep}$ and DIC inventories were similar at all sites and at site STL2 alone (Figure 7, Table 6). However, NH_4^+ and PO_4^{3-} increased considerably more with increasing $(SO_4^{2-})_{Dep}$ inventories at the STL2 site compared to other sites (Figure 7). Estimates of the C:N ratio of organic matter undergoing mineralization at the STL2 site from $(SO_4^{2-})_{Dep}$ and DIC inventories to NH_4^+ inventories and POC to PON inventories (Table 6) were significantly lower (3.4–5.3) than at the other sites (7.5–10) for all three types of estimates ($p < 0.05$). Estimates of the C:P ratio were more variable and were not significantly different (Table 6). The advection of nutrient-rich septic water from the upland may play a role in increasing nutrient inventories at the STL2 site, but the close coupling of NH_4^+ with DIC and $(SO_4^{2-})_{Dep}$ (Figure 7, Table 6) and the POC to PON data (Table 6) suggests microbial processing of N-rich organic matter *in situ*. The significantly higher inventories of DIC and $(SO_4^{2-})_{Dep}$ (Figure 5) and measured SO_4^{2-} reduction rates (Table 5, Figure 11) provide further evidence that these patterns result from more than simply increased inorganic nutrient inputs.

Septic waste contains high concentrations of DOC (Ptacek 1998), and although DOC inventories were not significantly higher at the STL2 site than other sites due to variability between dates, DON pools were significantly elevated at the STL2 site ($p < 0.05$; Figure 5). We hypothesize that N- (and possibly P-rich) labile septic-derived DOM from the upland stimulated the coupled fermentative and SO_4^{2-} reducing community at this site. The stimulation of microbial sulfate reduction and mineralization of this N-rich DOM resulted in increased porewater inventories of NH_4^+, DIC and $(SO_4^{2-})_{Dep}$. Stimulation of benthic and water-column primary production in the estuary by

nutrient inputs from the upland may have also provided additional organic matter for metabolism in these sediments. Advection of nutrient-rich septic-influenced water from the upland also likely contributed to the higher NH_4^+ and PO_4^{3-} inventories. On-going work is addressing this hypothesis directly.

Inorganic N:P ratios

The increasing NH_4^+:PO_4^{3-} ratios of porewater pools with higher $(SO_4^{2-})_{Dep}$ inventories (Figure 9) suggests either that the N:P ratio of the organic matter undergoing mineralization changed with the rate of metabolism (i.e., seasonally), H_2S mediated reductive dissolution of iron-phosphate minerals released PO_4^{3-} into porewaters when sulfate reduction and concurrent H_2S production rates were higher (Canfield et al. 1993), or nitrification–denitrification preferentially removed nitrogen from the sediments relative to phosphorus, particularly when SO_4^{2-} reduction rates were low. It is tempting to consider the removal of nitrogen via denitrification at lower overall rates of sediment metabolism as (discussed above) NO_x inventories were higher when $(SO_4^{2-})_{Dep}$ inventories were lower (Table 4). NH_4^+:PO_4^{3-} inventory ratios were quite low when $(SO_4^{2-})_{Dep}$ was low, falling well below the Redfield (1958) ratio of 16 (Figure 9), again indicating that NH_4^+ may have been removed via coupled nitrification–denitrification. The inhibitory effects of H_2S produced from SO_4^{2-} reduction on nitrification (Joye and Hollibaugh 1995) when SO_4^{2-} reduction rates were high [i.e. high $(SO_4^{2-})_{Dep}$] may account for this trend in NH_4^+:PO_4^{3-} ratios.

System-scale patterns of porewater creek-bank DOM

DOC and DON concentrations were higher than most previous studies have reported for coastal sediments. DOC and DON in excess of 10 mM and 500 μM, respectively, were often measured at depth in the sediment porewater (Figure 3). We examined intertidal sediment DOM in relatively small tidal creeks, and are unaware of any published DOM data from similar systems. Coastal subtidal marine sediment DOC concentrations of generally <3 mM (Burdige 2001) and DON <200 μM (Burdige and Zheng 1998) have been observed in Chesapeake Bay. Cape Lookout Bight porewater DOC reached concentrations of 10 mM in the summer, although concentrations were generally <5 mM (Alperin et al. 1994). Continental margin sediment DOC concentrations are typically lower, with <3 mM DOC off North Carolina (Alperin et al. 1999) and <1 mM in California margin sediments (Burdige et al. 1999). A study of sandy sediments in an estuarine lagoon found DON concentrations in excess of 100 μM (Yamamuro and Koike 1998), and DON in sediments of the Northern Adriatic approached 400 μM (Cermelj et al. 1997), which were similar to the DON concentrations presented here.

Burdige and Zheng (1998) observed a positive correlation between mineralization rates and DOC and DON concentrations, such that concentrations of

the dissolved organics were highest in the summer. Similarly, DOC production during summer was observed in Cape Lookout Bight sediments (Alperin et al. 1994). However, in the present study DOC and DON concentrations were not correlated with temperature (Table 3), and did not appear to vary seasonally. Profiles were obtained over a range of seasons (Table 2), and the data do not show seasonal accumulation of dissolved organics.

The relationships observed between $(SO_4^{2-})_{Dep}$, DIC, NH_4^+ and PO_4^{3-} porewater inventories (Figure 7, Tables 4 and 6) suggests a close coupling between SO_4^{2-} reduction and the terminal metabolic end-products of organic matter mineralization Figure 1, DIC, NH_4^+, PO_4^{3-}). However, there is a much less obvious coupling of $(SO_4^{2-})_{Dep}$ and DOC, presumably the substrate for SO_4^{2-} reduction in these sediments. $(SO_4^{2-})_{Dep}$ and DOC were not correlated at any of the sites except for surface 10 cm at SAP1 and deeper porewater at STL2 (Table 4), and there was no overall relationship when data from all sites was pooled (Figure 8). Similar regressions between DIC and DOC inventories yielded no significant results, with again the exception of the STL2 site ($p > 0.05$, data not shown).

DOC concentrations measured in these porewaters are the net result of both DOC production through hydrolytic breakdown of POM and transport of DOM into and out of the sediments, and the fermentative and terminal metabolic oxidation of DOM (Figure 1, Fenchel and Findlay 1995). In saltmarshes, plant root exudates can fuel SO_4^{2-} reduction independently of hydrolytic DOM production (Hines et al. 1999) and may contribute to the strong seasonal cycle of SO_4^{2-} reduction in saltmarshes coincident with the growing season (King 1988; Kostka et al. 2002b). Unvegetated intertidal creek-bank sediments are somewhat removed from this DOM exudate, and may rely more on the hydrolytic production of DOM from sediment POM.

The initial hydrolysis of POM can exceed the subsequent rates of fermentation and terminal metabolism, resulting in the accumulation of DOC in porewaters Arnosti and Repeta 1994; Brüchert and Arnosti 2003). However, it appears that production and mineralization of DOC may be more tightly coupled in intertidal creek-bank sediments, resulting in little change in the bulk DOC inventory. We speculate that the measured DOC represents a refractory pool of organic carbon that is largely unavailable for further microbial degradation. In this scenario, the labile DOC utilized by SO_4^{2-} reducers and by other terminal metabolizers is a small but rapidly cycled pool of DOC that is not detectable over or within the bulk pool. Measurements of specific organic compounds, such as acetate (Kostka 2002b) or ethanol (Hines et al. 1999), would potentially provide insight on the coupling of metabolic pathways in these sediments and such studies are planned for the future.

There was a significant positive relationship between DON and $(SO_4^{2-})_{Dep}$ inventories for data pooled from all the sites excluding STL2 (Table 4, Figure 8). The overall porewater inventories of DON are relatively low (around 5 μmol cm^{-2}) compared with inventories of other metabolites (Figure 5). The higher pools of DON associated with higher rates of SO_4^{2-}

reduction may be due to the coupling of DON production and terminal metabolism. In Chesapeake Bay sediments, Burdige and Zheng (1998) observed that, as rates of DOM utilization increased, consumption became non-selective and the C:N ratio of the DOM decreased, leading to a negative correlation between both the DOC and DON versus the DOC:DON ratio. It appears that there may be selective utilization of DON in sediments with lower SO_4^{2-} reduction rates (i.e. lower overall rates of metabolism) in this study as well. The DOC:DON inventory ratio decreased significantly with increasing $(SO_4^{2-})_{Dep}$, suggesting non-selective utilization of DOM at higher SO_4^{2-} reduction rates (Figure 9).

The hypothesis of selective utilization of DON at lower metabolic rates would require that the DIC:DIN ratio, as products of the mineralization of DOC and DON, mirror the DOC:DON ratio, i.e. the DIC:DIN would be low when metabolic rates are low due to the preferential mineralization of DON and production of DIN relative to mineralization of DOC and production of DIC. This is not the trend we observed. In contrast, the DIC:DIN ratio followed a pattern very similar to the DOC:DON ratio (Figure 9). Denitrification and the preferential removal of inorganic nitrogen relative to DIC alone would not account for this pattern. The decrease in DIC:DIN and DOC:DON ratios with increasing terminal metabolism must be driven, therefore, by fermentation and hydrolysis of particulate organic matter. During the summer, either preferential degradation of PON to DON compared with POC degradation, or a change in the organic matter source to more N-rich POM appears to be the mechanism driving the changes in DOC:DON and DIC:DIN ratios (Figure 9).

The POC and PON data (Table 5) from the STL2 and OKT4 sites, where a seasonal record was obtained, indicate that sediment POC:PON increased in the summer. The POC:PON ratio of inventories to 40 cm increased during the summer at both sites (Figure 10). The changing POC to PON ratios were used to estimate the C:N of the oxidized organic matter, and yielded estimates of 5.3 and 7.6 at site STL2 and OKT4, respectively (Table 6), similar to estimates based on $(SO_4^{2-})_{Dep}$ and DIC to NH_4^+ inventories. Although this may be due in part to changes in particulate organic matter inputs, the pattern suggests that preferential degradation of PON to DON by the hydrolytic bacterial community in the summer, rather than variable inputs of POM or preferential utilization of DON by terminal metabolizers, exerted overall control on the DOC:DON and DIC:DIN ratios in these sediments (Figure 9).

The apparent hydrolytic control of the C:N ratio, along with the lack of seasonal accumulation of porewater DOC (Table 3) and the weak seasonal trend in SO_4^{2-} reduction rates (Table 5) and terminal metabolite porewater inventories (Table 3), suggests that the overall mineralization of organic matter is limited by the initial hydrolysis of POM. Controls on the hydrolytic/fermentative/terminal metabolic organic matter-oxidizing microbial consortium in sediments remain an unclear, representing an important avenue for future research.

Summary

The large dataset obtained through the use of porewater equilibration samplers at eight intertidal estuarine sites allowed us to evaluate system-scale seasonal and spatial patterns of sediment metabolism, with an emphasis on the role of DOC and DON. We have come to the following conclusions:

(1) Seasonality was observed, suggesting temperature does in part control rates of organic matter oxidation in unvegetated intertidal creekbank sediments. However, temperature alone cannot adequately describe the patterns of sulfate depletion, terminal metabolic products (DIC, NH_4^+, PO_4^{3-}), dissolved organic carbon and nitrogen, and sulfate reduction observed.
(2) There were significant system-scale correlations between the inorganic products of terminal metabolism (DIC, NH_4^+ and PO_4^{3-}) and sulfate depletion, and sulfate reduction appeared to be the dominant terminal carbon oxidation pathway in these sediments. The carbon to nitrogen stoichiometry of the organic matter undergoing mineralization across these sites was estimated to be 7.5–10.
(3) The data suggest that septic-derived waste from a residential community in the developed upland provided N-rich labile DOM (with a C:N ratio of 3.4–5.3) that stimulated rates of metabolism at the STL2 site, as well as contributing to inorganic nutrient and DIC inventories via the advection of septic water.
(4) Hydrolytic production and fermentative and terminal metabolic consumption of labile DOC is closely coupled in these sediments. Bulk measurements of DOC did not aid in elucidating controls or pathways of carbon oxidation, and bulk DOC in these sediments is likely a recalcitrant pool. Terminal organic matter mineralization in these sediments appeared to be limited by hydrolytic/fermentative breakdown of POM and DOM when overall rates of metabolism were high. Hydrolysis also appears to control the C:N ratio of the POM and DOM. Controls on the breakdown of organic matter and the coupling between hydrolytic/fermentative and terminal metabolic bacterial communities is an important topic for future research.

Acknowledgments

We thank R. Lee, S. Carini, L. Velasquez, T. Roberts, and P. Olecki for help in the field and laboratory; W. Sheldon for providing Matlab mapping tools; and, C. Meile and three anonymous reviewers for providing comments that substantially improved this paper. This research was supported by the National Science Foundation's Georgia Coastal Ecosystems Long Term Ecological Research Program (OCE 99-82133) and National Oceanic and Atmospheric Administration Sea Grant Programs in Georgia (award numbers NA06RG0029-R/WQ11 and R/WQ12A) and South Carolina (award number: NA960PO113).

References

Aller R.C. and Aller J.Y. 1998. The effect of biogenic irrigation intensity and solute exchange on diagenetic reaction rates in marine sediments. J. Mar. Res. 56: 905–936.

Alperin M.J., Albert S.T.L2 and Martens C.S. 1994. Seasonal variations in production and consumption rates of dissolved organic carbon in an organic-rich coastal sediment. Geochim. Cosmochim. Acta 58: 4909–4930.

Alperin M.J., Martens C.S., Albert S.T.L2, Suayah I.B., Benninger L.K., Blair N.E. and Jahnke R.A. 1999. Benthic fluxes and porewater concentration profiles of dissolved organic carbon in sediments from the North Carolina continental slope. Geochim. Cosmochim. Acta 63: 427–448.

Álvarez-Salgado X.A. and Miller A.E.J 1998. Simultaneous determination of dissolved organic carbon and total dissolved nitrogen in seawater by high temperature catalytic oxidation: conditions for precise shipboard measurements. Mar. Chem. 62: 325–333.

Amon R.M.W. and Benner R. 1996. Bacterial utilization of different size classes of dissolved organic matter. Limnol. Oceanogr. 41: 41–51.

Arnosti C. and Repeta D.J. 1994. Oligosaccharide degradation by anaerobic marine bacteria: characterization of an experimental system to polymer degradation in sediments. Limnol. Oceanogr. 39: 1865–1877.

Boudreau B.P. 1997. Diagenetic Models and their Implications. Springer, Berlin.

Boynton W.R. and Kemp W.M. 1985. Nutrient regeneration and oxygen consumption by sediments along an estuarine salinity gradient. Mar. Ecol. Prog. Ser. 23: 45–55.

Brüchert V. and Arnosti C. 2003. Anaerobic carbon transformation: experimental studies with flow-through cells. Mar. Chem. 80: 171–183.

Burdige D.J. and Martens C.S. 1988. Biogeochemical cycling in an organic-rich coastal marine basin: 10. The role of amino acids in sedimentary carbon and nitrogen cycling. Geochim. Cosmochim. Acta 52: 1571–1584.

Burdige D.J. and Gardner K.G. 1998. Molecular weight distribution of dissolved organic carbon in marine sediment pore waters. Mar. Chem. 62: 45–64.

Burdige D.J. and Zheng S. 1998. The biogeochemical cycling of dissolved organic nitrogen in estuarine sediments. Limnol. Oceanogr. 43: 1796–1813.

Burdige D.J., Berleson W.M., Coale K.H., McManus J. and Johnson K.S. 1999. Fluxes of dissolved organic carbon from California continental margin sediments. Geochim. Cosmochim. Acta 63: 1507–1515.

Burdige D.J. 2001. Dissolved organic matter in Chesapeake Bay sediment pore waters. Org. Geochem. 32: 487–505.

Canfield D.E., Raiswell R., Westrich J.T., Reaves C.M. and Berner R.A. 1986. The use of chromium reduction in the analysis of reduced inorganic sulfur in sediments and shales. Chem. Geol. 54: 149–155.

Canfield D., Thamdrup B. and Hansen J. 1993. The anaerobic degradation of organic matter in Danish coastal sediments: Iron reduction, manganese reduction, and sulfate reduction. Geochim. Cosmochim. Acta 57: 3867–3883.

Capone D.G. and Kiene R.P. 1988. Comparison of microbial dynamics in marine and fresh-water sediments - contrasts in anaerobic carbon catabolism. Limnol. Oceanogr. 33: 725–749.

Cermelj B., Bertuzzi A. and Faganeli J. 1997. Modeling of pore water nutrient distribution and benthic fluxes in shallow coastal waters (Gulf of Trieste, Northern Adriatic). Water Air Soil Pollut. 99: 435–444.

Enoksson V. 1993. Nutrient recycling by coastal sediments: effects of added algal material. Mar. Ecol. Prog. Ser. 92: 245–254.

Fenchel T.M. and Findlay B.J. 1995. Ecology and evolution of anoxic worlds. Oxford University Press, Oxford.

Froelich P.N., Klinkhammer G.P., Bender M.L., Luedtke N.A., Heath G.R., Cullen D., Dauphin P., Hammond D., Hartman B. and Maynard V. 1979. Early oxidation of organic-matter in

pelagic sediments of the eastern equatorial Atlantic – suboxic diagenesis. Geochim. Cosmochim. Acta 43: 1075–1090.

Hesslein R.H. 1976. An in situ sampler for close interval pore water studies. Limnol. Oceanogr. 21: 912–914.

Hines M.E., Evans R.S., Genthner B.R.S, Willis S.G., Friedman S., Rooney-Varga J.N. and Devereux R. 1999. Molecular phylogenetic and biogeochemical studies of sulfate-reducing bacteria in the rhizosphere of *Spartina alterniflora*. Appl. Environ. Microbiol. 65: 2209–2216.

Hopkinson C.S. 1987. Nutrient regeneration in shallow-water sediments of the estuarine plume region of the nearshore Georgia Bight, USA. Mar. Biol. 94: 127–142.

Hopkinson C.S., Giblin A.E., Tucker J. and Garritt R.H. 1999. Benthic metabolism and nutrient cycling along an estuarine salinity gradient. Estuaries 22: 825–843.

Howarth R.W. 1988. Nutrient limitation of net primary production in marine ecosystems. Ann. Rev. Ecol. 19: 89–110.

Howarth R.W. 1993. Microbial processes in salt-marsh sediments. In: Ford T.E. (ed.), Aquatic microbiology: an ecological approach. Blackwell, Cambridge, pp. 239–259.

Iversen N. and Jørgensen B.B. 1985. Anaerobic methane oxidation rates at the sulfate-methane transition in marine sediments from Kattegat and Skagerrak (Denmark). Limnol. Oceanogr. 30: 944–955.

Jørgensen B.B. 1977. Sulfur cycle of a coastal marine sediment (Limfjorden, Denmark). Limnol. Oceanogr. 22: 814–832.

Jørgensen B.B. 1978. A comparison of methods for the quantification of bacterial sulfate reduction in coastal marine sediments. 1. Measurements with radiotracer techniques. Geomicrobiol. J. 1: 11–27.

Jørgensen B.B. 1982. Mineralization of organic-matter in the sea bed – the role of sulfate reduction. Nature 296: 643–645.

Jørgensen B.B. and Sørensen J. 1985. Seasonal cycles of O_2, NO_3^- and SO_4^{2-} reduction in estuarine sediments: the significance of an NO_3^- reduction maximum in spring. Mar. Ecol. Prog. Ser. 24: 65–74.

Jørgensen B.B. 2000. Bacteria and marine biogeochemistry. In: Schulz H.D. and Zabel M. (eds), Marine geochemistry. Springer, New York, pp. 173–207.

Joye S.B. and Hollibaugh J.T. 1995. Influence of sulfide inhibition of nitrification on nitrogen regeneration in sediments. Science 270: 623–624.

King G.M. 1988. Patterns of sulfate reduction and the sulfur cycle in a South Carolina salt marsh. Limnol. Oceanogr. 33: 376–390.

Kostka J.E., Gribsholt B., Petrie E., Dalton D., Skelton H. and Kristensen E. 2002a. The rates and pathways of carbon oxidation in bioturbated saltmarsh sediments. Limnol. Oceanogr. 47: 230–240.

Kostka J.E., Roychoudhury A. and Van Cappellen P. 2002b. Rates and controls of anaerobic microbial respiration across spatial and temporal gradients in saltmarsh sediments. Biogeochemistry 60: 49–76.

Lomstein B.A., Blackburn T.H. and Henriksen K. 1989. Aspects of nitrogen and carbon cycling in the northern Bering Shelf sediment I. The significance of urea turnover in the mineralization of NH_4^+. Mar. Ecol. Prog. Ser. 57: 237–247.

Lowe K.L., DiChristina T.J., Roychoudhury A.N. and Van Cappellen P. 2000. Microbiological and geochemical characterization of microbial Fe(III) reduction in salt marsh sediments. J. Geomicrobiol. 17: 163–178.

Marvin-DiPasquale M.C., Boynton W.R. and Capone D.G. 2003. Benthic sulfate reduction along the Chesapeake Bay central channel. II. Temporal controls. Mar. Ecol. Prog. Ser. 260: 55–70.

Meile C., Koretsky C.M. and Van Cappellen P. 2001. Quantifying bioirrigation in aquatic sediments: an inverse modeling approach. Limnol. Oceanogr. 46: 164–177.

Middelburg J.J., Soetart K. and Herman P.M.J 1997. Empirical relationships for use in global diagenetic models. Deep-Sea Res. 44: 327–344.

Moore J.W., Schindler D.E., Scheuerell M.D., Smith D. and Frodge J. 2003. Lake eutrophication at the urban fringe, Seattle region, USA. Ambio 32: 13–18.

Murphy J. and Riley J.P. 1962. A modified single solution method for the determination of phosphate in natural systems. Anal. Chim. Acta 27: 31–36.

Nielsen O.I., Kristensen E. and Macintosh D.J. 2003. Impact of fiddler crabs (*Uca* spp) on rates and pathways of benthic mineralization in deposited mangrove shrimp pond waste. J. Exp. Mar. Biol. Ecol. 289: 59–81.

Pilson M.E.Q. 1998. An introduction to the chemistry of the sea. Prentice Hall, New Jersey.

Ptacek C.J. 1998. Geochemistry of a septic-system plum in a coastal barrier bar, Point Pelee, Ontario, Canada. J. Cont. Hydrol. 33: 293–312.

Redfield A.C. 1958. The biological control of chemical factors in the environment. Am. Sci. 46: 205–222.

Roden E.E. and Wetzel R.G. 1996. Organic carbon oxidation and suppression of methane production by microbial Fe(III) oxide reduction in vegetated and unvegetated freshwater wetland sediments. Limnol. Oceanogr. 41: 1733–1748.

Rosenfeld J.K. 1979. Ammonium adsorption in anoxic nearshore sediments. Limnol. Oceanogr. 24: 356–364.

Rowe G.T., Clifford C.H. and Smith K.L. 1976. Benthic nutrient regeneration and its coupling to primary productivity in coastal waters. Nature 255: 215–217.

Roychoudhury A.N., Viollier E. and Van Cappellen P. 1998. A plug flow-through reactor for studying biogeochemical reactions in undisturbed aquatic sediments. Appl. Geochem. 13: 269–280.

Rysgaard S., Thastum P., Dalsgaard T., Christensen O.K.T2 and Sloth N.P. 1999. Effects of salinity on NH_4^+ adsorption capacity, nitrification, and denitrification in Danish estuarine sediments. Estuaries 22: 21–30.

Sansone F.J. and Martens C.S. 1978. Methane oxidation in Cape Lookout Bight, North Carolina. Limnol. Oceanogr. 23: 349–355.

Sarazin G., Michard G. and Prevot F. 1999. A rapid and accurate spectroscopic method for alkalinity measurements in sea water samples. Water Res. 33: 290–294.

Seitzinger S.P. 1988. Denitrification in freshwater and coastal marine ecosystems: ecological and geochemical significance. Limnol. Oceanogr. 33: 702–724.

Solorzano L. 1969. Determination of ammonia in natural waters by the phenolhypochlorite method. Limnol. Oceanogr. 14: 799–801.

Stookey L.L. 1970. Ferrozine – a new spectrophotometric reagent for iron. Anal. Chem. 42: 779–781.

Stumm W. and Morgan J.J. 1996. Aquatic Chemistry, 3rd ed. Wiley, New York.

Sundareshwar P.V. and Morris J.T. 1999. Phosphorus sorption characteristics of intertidal marsh sediments along an estuarine salinity gradient. Limnol. Oceanogr. 44: 1693–1701.

Teal J.M. 1958. Distribution of fiddler crabs in Georgia salt marshes. Ecology 39: 185–193.

Westrich J.T. and Berner R.A. 1988. The effect of temperature on rates of sulfate reduction in marine sediments. Geomicrobiol. J. 6: 99–117.

Yamamuro M. and Koike I. 1998. Concentrations of nitrogen in sandy sediments of a eutrophic estuarine lagoon. Hydrobiologia 386: 37–44.